PILOT SCALE TRIALS ON ATMOSPHERIC FLUIDIZED BED COMBUSTION OF A SASKATCHEWAN PETROLEUM COKE

CONTRACT SERIAL NO. OST84-00512
REQUISITION NO. 23440-5-9015
CONTRACTOR: QUEEN'S UNIVERSITY

H.A. Becker, R.K. Code and J.R. Stephenson
Department of Chemical Engineering
Queen's University at Kingston
Kingston, Canada K7L 3N6

A report to
Energy, Mines and Resources Canada
Energy Research Laboratories, CANMET
Ottawa, Canada

Technical Report QFBC.TR.87.5
Queen's Fluidized Bed Combustion Laboratory

64 pp

MICROMEDIA

ABSTRACT

Trials on the burning of a petroleum coke, a residue of the processing of Alberta light crude oil, were performed in an atmospheric fluidized bed combustion (AFBC) pilot plant. Sand, mean particle dia. 0.6 mm, was usually used as the bed material but several trials with limestone, mean particle dia. 0.83 mm, were also performed. Other conditions of the trials were mean coke particle dia., 0.28 mm; fluidizing velocity, 1.1--1.9 m/s; excess air, up to 15 %; cyclone recycle ratio (fraction of cyclone catch recycled), 0--1; and bed temperature, 833--1005 °C. The combustion efficiency as measured by carbon burnup was 65--99 %. Correlation of combustion efficiency with the operating variables demonstrates close similarity with the burning of Syncrude coke. Although sand beds were used in most of the work, substantial sulphur "capture" was nevertheless generally observed. The data show that this is due to sulphur retention and concentration in the unburnt char. The S/C mole ratio of the char can be as high as three times that of the fuel. The sometimes significant role of char in sulphur transport is one of the principal findings of the present work. Nitric oxide emissions were ordinary for AFBC, showing 8--29 % conversion of fuel nitrogen to NO. The work covered an unusually extended range of the cyclone recycle ratio r, right up to r = 1 (total recycle of cyclone catch). In correlating combustion efficiency, it was found that the ratio r inadequately characterizes the effects of recycle at r > 0.90. The overhead recycle ratio R, the fraction of cyclone catch plus baghouse catch that is recycled, serves much better and indeed appears to be wholly adequate. This is the second major finding of the work.

Notation

Subscripts (codes for material streams):

a	combustion air
b	bed product (bed solids removed directly from the bed, here by overflow from the top or by mechanical extraction from the side near the bottom)
c	cyclone product (cyclone catch not recycled)
d	cycloned solids (dust catch in cyclone)
e	elutriated solids (cycloned solids d plus baghouse product h)
f	fuel (here petroleum coke)
g	stack gas
h	baghouse product (here equals baghouse catch, none of which was recycled)
m	m'th material stream
n	n'th material stream
o	overhead product solids (cyclone c plus baghouse h)
p	total product solids (bed b plus cyclone c plus baghouse h)
r	recycled cycloned solids
s	"stone"; solids fed to form a stable bed and possibly to act as a sulphur sorbent, here sand (inert) and limestone (sorbent)
st	at stoichiometric conditions in respect to fuel/air ratio

Variables:

a_i	i = 1, 2, ...; coefficients in multiple linear regression model
A_b	cross-sectional area of bed, m^2
C	$= \ln^{-1} a_o$, proportionality constant from multiple linear regression model

D_p	particle diameter, m; here defined by sieve analysis (D_p = mesh size)
$\hat{D}_p$	mass-median particle diameter for a population of particles of mixed size; $D_p = \hat{D}_p$ at $F_D = 1/2$
F_D	$= F_D(D_p)$, particle-size distribution function, the mass fraction of diameter smaller than D_p; the "mass fraction undersize"
H	effective bed height or depth as indicated by the pressure distribution along the bed wall, m
m	mass of material, kg
m_b	bed mass (holdup), kg
$\dot{m}$	mass flux of material, kg/h
$\dot{n}$	molar flux of material, kmol/h
n_t	number of in-bed cooling tubes
Q_b	= heat flux out of bed, W
r	$= \dot{m}_r/\dot{m}_d = \dot{m}_r/(\dot{m}_r + \dot{m}_c)$ = cyclone recycle ratio, fraction of cyclone catch that is recycled
R	$= \dot{m}_r/\dot{m}_c = \dot{m}_r/(\dot{m}_r + \dot{m}_c + \dot{m}_h)$ = overhead recycle ratio, fraction of cyclone and baghouse catches that is recycled
T	temperature, K
T_b	bed temperature, K
v	superficial gas velocity up the combustor, m/s, also called the fluidizing velocity; measured at the bed temperature, freeboard pressure, and exhaust gas composition
W_i	mass ratio of component i in a material sample or stream, here the mass fraction d.b. (dry basis), the mass of i per unit mass of dry matter
ϵ_a	$= \phi_a - 1$, the excess air level
η_C	carbon combustion efficiency, fraction of fuel carbon converted into gaseous products
η_{cyc}	$= \dot{m}_d/\dot{m}_e = (\dot{m}_r + \dot{m}_c)/(\dot{m}_r + \dot{m}_c + \dot{m}_h)$ = cyclone efficiency
η_S	sulphur-capture efficiency, fraction of fuel sulphur not converted into gaseous products

τ_b = $m_b/\dot{m}_b$, estimate of residence time of bed product in the combustor, h

τ_p = $m_b/\dot{m}_p$, estimate of mean residence time of solids in the combustor, h

ϕ_a = $\dot{n}_a/\dot{n}_{a,st}$, air equivalence ratio; air supplied for combustion divided by stoichiometric air requirement of fuel

$\phi_{i,mm}$ = $\dot{m}_{i,m}/\dot{m}_{i,n}$, mass flux ratio of component i in the m'th and n'th material streams

ξ_{NO} conversion factor of fuel nitrogen to nitric oxide

Acronyms:

AFBC atmospheric fluidized bed combustion

ERL Energy Research Laboratories, CANMET, Energy, Mines & Resources Canada

QFBC Queen's Fluidized Bed Combustion Laboratory

PREFACE

This is the final report on one of the tasks performed under a contract with Supply and Services Canada (DSS) under the auspices of the Canada Center for Mineral and Energy Technology (CANMET), Energy, Mines and Resources Canada:

DSS Contract Serial No.: OST84-00512

Title: A Program of Pilot Scale R&D on Bubbling-Bed Atmospheric Fluidized Bed Combustion

Principal Investigators: Dr. H.A. Becker and Dr. R.K. Code, Department of Chemical Engineering, Queen's University at Kingston, Kingston, Ontario K7L 3N6
Telephone: (613) 545-2767

Scientific Authority: Dr. E.J. Anthony, Building 1, Energy Research Laboratories, CANMET, Haanel Drive, Bells Corners, Ontario
Postal address: Energy Research Laboratories, CANMET 555 Booth Street, Ottawa, Ontario K1A 0G1
Telephone: (613) 996-4570, ext. 185

Commencement date: April 1, 1985

Delivery date: March 31, 1987

Consignee: Energy, Mines and Resources, Energy Research Laboratories, CANMET, 555 Booth Street, Ottawa, Ontario K1A 0G1

Science Procurement Manager: Ms. J.P.S. Sztramko, Science Branch, Supply and Services Canada, Place du Portage, Phase III, 11 Laurier Street, Hull, Quebec K1A 0D5

1. Introduction

The present work is another in a series of investigations of the burning of Canadian candidate fuels by atmospheric fluidized bed combustion (AFBC) in the Queen's University AFBC pilot plant under DSS contracts sponsored by Energy, Mines and Resources Canada. Fuels examined under previous contracts (Becker & Code 1983; Becker, Code, McCleave & Stephenson 1985) were Eastern Canadian sub-bituminous coals (Minto, Devco and Evans), an Appalachian coal (Kentucky No. 9), and Syncrude coke. The present contract included further studies of Eastern Canadian sub-bituminous coals (Minto, Devco Prince, Evans and Lingan), and first studies of Western anthracite coal (Mt. Klappan), a Western sub-bituminous coal (Highvale), a coal-water slurry (with Devco coal), and a petroleum coke. Reports have been issued on the anthracite trials (Becker, Code & Stephenson 1987a) and the Highvale trials (Becker, Code & Stephenson 1987b). The present report concerns the work on the petroleum coke.

Coke is commonly a by-product in petroleum refining and upgrading; it can also be a main product in processes making coke for applications such as manufacture of carbon electrodes. As a by-product, an attractive application may be to obtain part or all of the process energy requirements of a plant by combustion of the coke. Because of the small particle size and very low volatile content of this fuel, the only process well capable of burning it is fluidized bed combustion. For this reason, by-product cokes are likely candidates for early commercial application of FBC in Canada. This was one of the motivations for the present work. We had already (Becker, et al. 1985; Anthony, et al. 1985; Anthony, et al. 1987) studied the burning of Syncrude coke, the residue from processing oil sands at the Syncrude plant at Fort McMurray, Alberta. Anthony, Desai & Friedrich (1982), using a smaller pilot plant AFBC combustor, also studied the burning of Suncor coke, the residue of oil-sands processing by another scheme at the Suncor plant at Fort

McMurray. The Suncor coke appears to have significantly different combustion behaviour from the Syncrude. The present coke, quite different in origin, is a by-product of processing a light Alberta crude oil. The results, taken together with those on the Syncrude and Suncor cokes, should indicate the range of combustion behaviour in AFBC to be found in Canadian by-product cokes and should underscore the similarities and differences.

It was also intended to use the present coke in basic studies of char residence time in the pilot plant combustor. This project collapsed because of loss of the key team member who had to leave before the research was well started. The focus of the present report is thus confined to the overall combustion performance of the coke. The principal objectives were to determine the effects of the operating parameters on combustion efficiency, sulphur dioxide emission and nitric oxide emission. The parameters varied were bed temperature, fluidizing velocity, recycle of elutriated solids, excess air level, and the basic bed material (sand or limestone).

2. The pilot plant

The pilot plant, illustrated in Fig. 2.1, has been described in detail by Becker & Code (1982). The combustor is square in cross-section, 0.155 m^2 in area. The height from distributor plate to end of freeboard is 4 m. Cooling tubes inserted in the bed provide the cooling load and the primary control on bed temperature. The gas exhaust train includes a cyclone separator and a baghouse. Solids from the cyclone may be partly or wholly recycled to improve combustion efficiency.

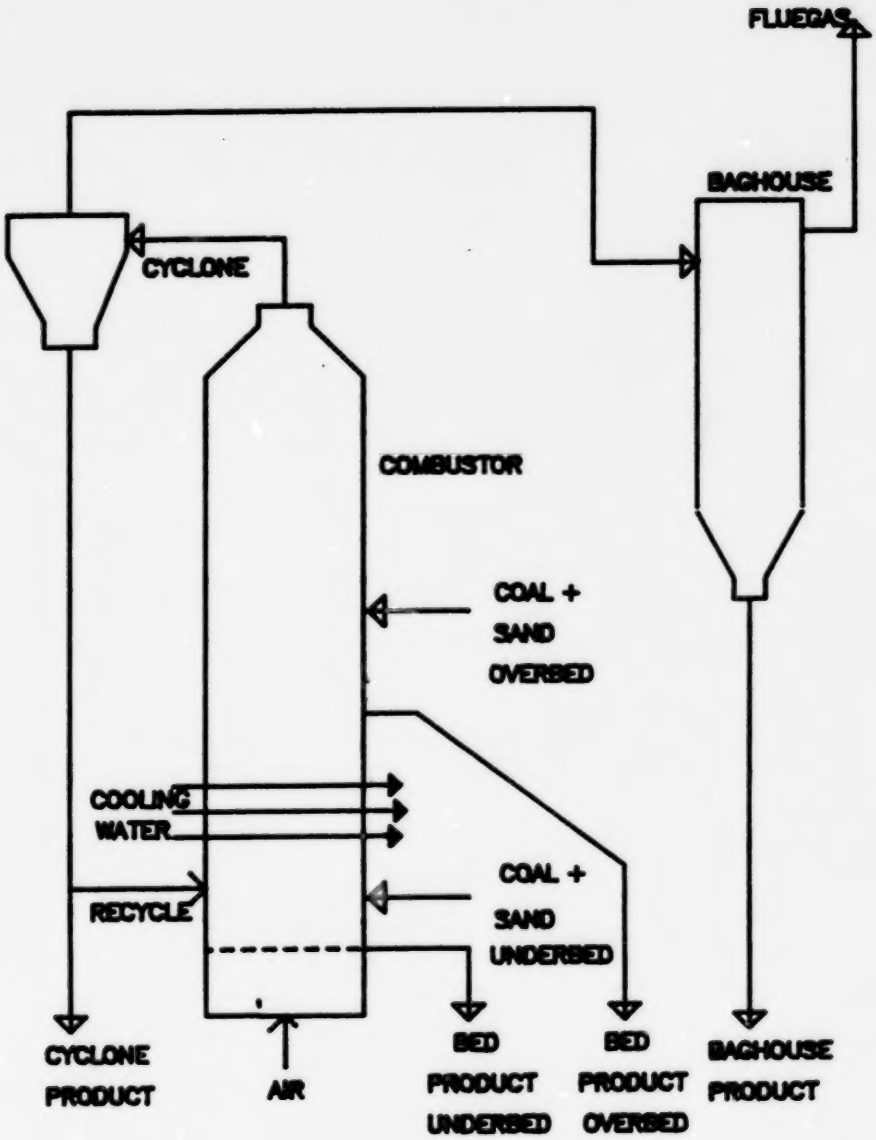

Fig. 2.1 The pilot plant

3. Materials

3.1 The coke

The subject petroleum coke is the product of a delayed coking process at the Consumers Co-op Refinery at Regina, Saskatchewan. The feed material was light Alberta crude oil. The coke is a by-product but is of anode grade and has a ready market. The chemical analysis of the coke, Table 3.1, shows a low ash content, high fixed carbon, and a moderate amount of sulphur. The ash analysis, Table 3.1, shows a significant proportion of CaO; however, because the ash content is so low, the sulphur-capture potential of this Ca is small. The fuel Ca/S mole ratio is 0.052.

The particle size analysis of the coke as fired is shown in Table 3.2 and Fig. 3.1. The mass-median particle diameter is 0.278 mm; 80 % is under 0.48 mm and 20 % is under 0.107 mm. This fuel is comparable in particle size with the Syncrude coke used in an earlier study, mass-median diameter 0.26 mm.

3.2 The stone material

"Stone" is normally used to provide a stable fluidized bed of particles which acts as a vehicle for the combustion process. Sand is usually used when sulphur capture is not important; it is essentially inert in the process. When sulphur capture is sought, limestone is employed and acts both as SO_2 sorbent and bed stabilizer.

In the present trials, most runs were done with a silica sand, mass-median dia. 0.60 mm, but some were carried out with a Western (Athabasca) limestone, mass-median dia. 0.83 mm. The particle size distribution of the sand is shown in Fig. 3.2. The limestone was also used in the Syncrude trials and has been

Table 3.1. Chemical analysis of petroleum coke from the Consumers Co-op Refinery, Regina. Results expressed in weight percent, dry (moisture-free) basis, except for HHV. Acronyms:

VCM	volatile combustible matter
FC	fixed carbon
HHV	higher heating value
MAF	moisture- and ash-free basis
QAFBC	Queen's AFBC Laboratory
ERL	Energy Research Laboratories, CANMET

Analysis	Results		
	Reporter	QAFBC	ERL
Proximate/ultimate	Moisture	8.43*	0.22
	Ash	1.07	0.63
	VCM	9.99	10.49
	FC	88.95	88.88
	C	92.91	91.82
	H	4.85	3.63
	N	1.15	1.34
	S	2.91	2.71
	O	0.00	0.00
Sulphur forms	total		2.60
	organic		2.55
	pyritic		0.04
	sulphate		0.01
Ash	SiO_2		36.3
	Al_2O_3		4.93
	Fe_2O_3		6.38
	TiO_2		0.37
	P_2O_5		0.42
	CaO		24.56
	MgO		2.40
	SO_3		18.76
	Na_2O		1.29
	K_2O		0.49
	BaO		0.12
	SrO		0.03
	LOF		3.95
	total		100.00
Heating value, MJ/kg MAF	HHV	35.19	36.32

* Moisture as received; the coke was dried to 1.5 % moisture for the coke/limestone trials.

Table 3.2. Tyler-sieve particle size analysis of petroleum coke from the Consumers Co-op Refinery, Regina

Sieve No.	Opening, mm	Mass % undersize	
		Run 860606	Run 860605
7/16	11.20	100.00	--
3/8	9.51	99.88	--
5/16	8.00	99.88	--
1/4	6.35	99.62	--
4	4.76	99.42	--
5	4.00	99.21	99.22
6	3.36	98.88	98.94
7	2.83	98.32	98.36
8	2.38	97.77	97.77
10	2.00	97.08	97.09
12	1.68	96.24	96.29
14	1.41	95.37	95.43
16	1.19	94.29	94.31
18	1.00	93.29	93.32
20	0.841	92.19	92.23
25	0.707	90.81	90.83
30	0.595	87.60	87.75
35	0.500	81.28	81.56
40	0.420	72.77	73.02
45	0.354	61.95	61.94
50	0.297	53.25	53.07
60	0.250	45.22	44.88
70	0.210	39.06	38.65
80	0.177	33.51	33.08
100	0.149	28.21	27.74
120	0.125	23.70	23.21
140	0.105	19.83	19.45
170	0.088	16.95	16.51
200	0.074	14.51	14.07
230	0.063	11.99	11.74
270	0.053	9.64	8.11
325	0.044	7.64	5.73
400	0.037	6.64	5.01

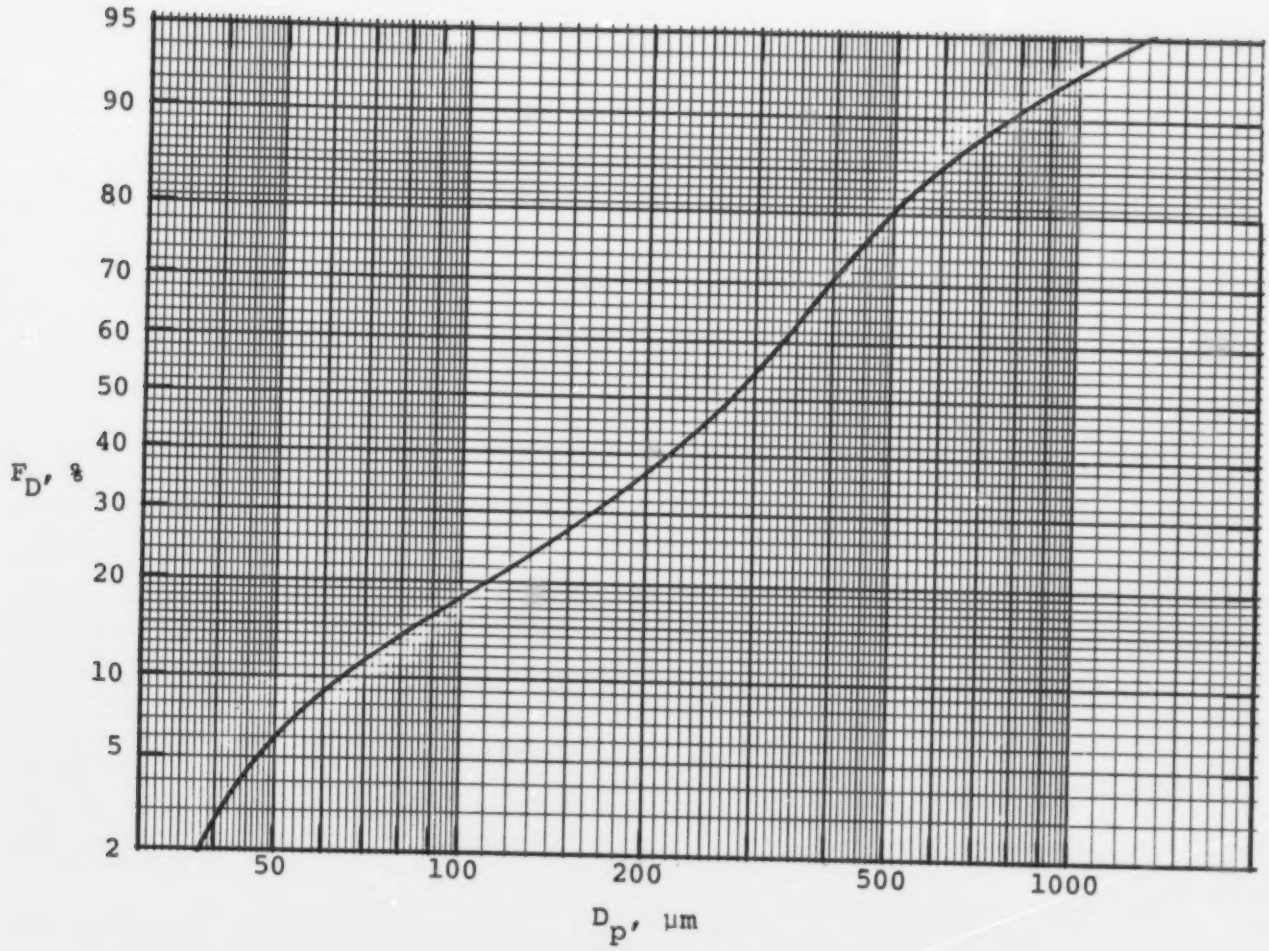

Fig. 3.1 Particle size distribution of the petroleum coke by sieve analysis: mass fraction undersize vs particle diameter indicated by sieve opening

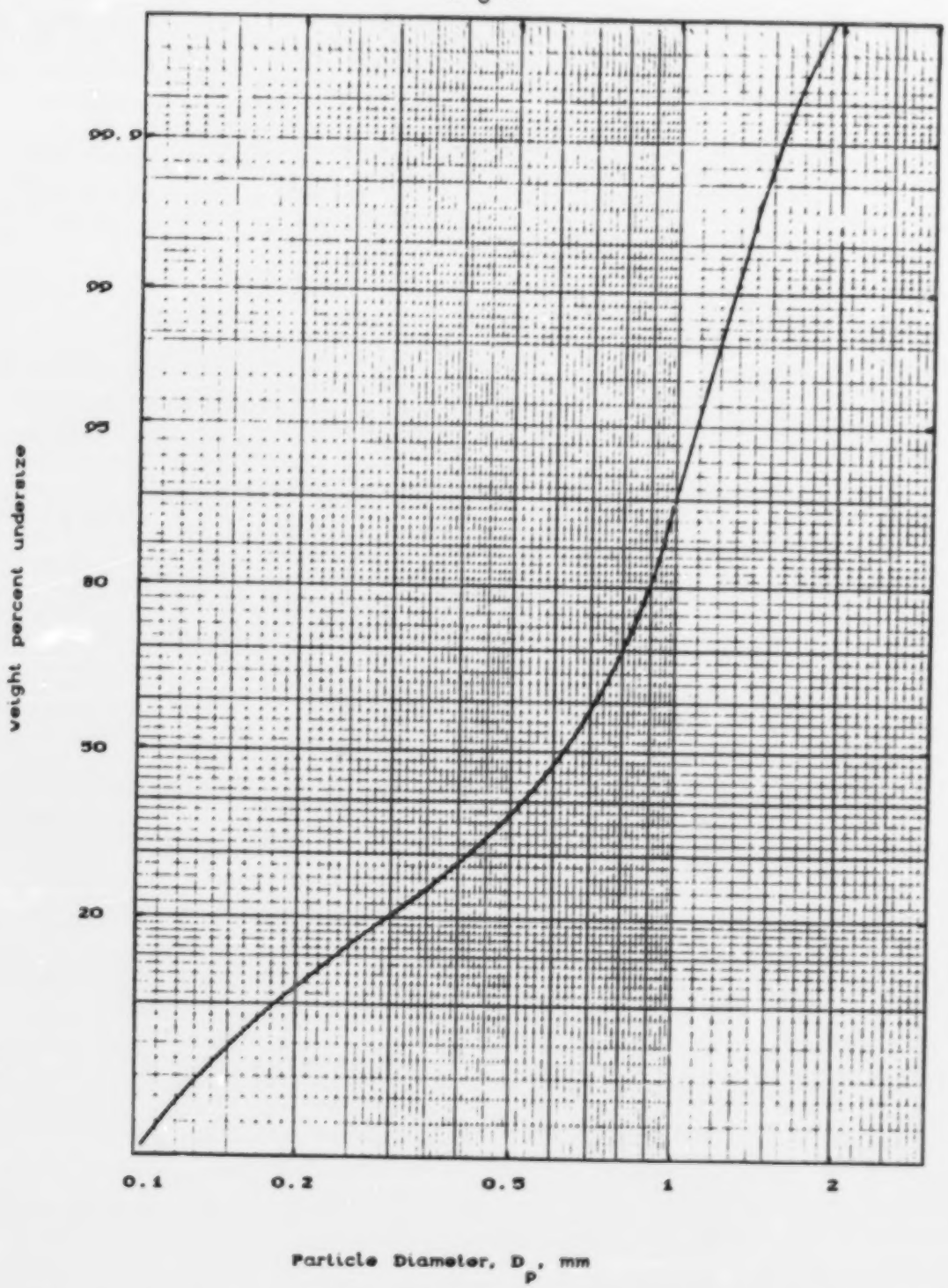

Fig. 3.2 Particle size distribution of the Kingston sand by sieve analysis: mass fraction undersize vs particle diameter indicated by sieve opening

described in the related reports (Becker, et al. 1985; Anthony, et al. 1987).

4. Operating conditions

The operating conditions of the fourteen successful trials are given in Table 4.1.

Our work on Syncrude coke (Becker, et al. 1985; Anthony, et al. 1987) indicated that high temperatures might be required for good combustion efficiency, so bed temperatures up to 1000 °C were used; in burning sub-bituminous coal, by contrast, temperatures of 800--900 °C are normally adequate.

When operating with sand beds, a moderate continuous feed of sand was used to maintain the bed and provide a steady flow of bed product. Since the sand is inert, this approach is in industrial practice unnecessary and wasteful of the sand; all that is really needed is to supply replacement sand in the quantity needed to compensate for elutriation losses and thus maintain a constant bed depth. However, since the loss of sand from the bed in this mode is of small particles only, it takes longer to fully establish a steady-state distribution of particle size in the bed, and for this reason we chose to operate with substantial overflow. In operation with limestone, the stone feedrate determines the Ca/S ratio and two levels of feedrate were used to obtain values of Ca/S of 2 and 4.

Excess air levels were regulated primarily through the exhaust oxygen level which was maintained above zero and as high as 30 % of the oxygen fed. In cases with low combustion efficiency, this nevertheless sometimes resulted in negative excess air levels based on the air requirement for total combustion.

Table 4.1. Operating conditions of the trials

Trial	n_t	$\hat{D}_{pf}$, mm	$\dot{m}_f$, kg/h	$\hat{D}_{ps}$, mm	$\dot{m}_s$, kg/h	Ca/S*	$\dot{m}_a$, kg/h	ε_a %	r	R	T_b, °C	v, m/s	H cm	τ_p h	τ_b, h	COT h
					Sand											
860212	2	0.28	19.3	0.60	8.8	0	200	-9.9	0	0	833	1.13	37	8.4	25.5	11.4
860303	2		24.5		6.0		257	-9.1	0.797	0.780	852	1.48	37	6.6	11.4	10.0
860305	2		26.8		5.5		285	-7.7	0	0	905	1.72	37	9.4	49.1	10.0
860304	2		25.4		5.4		311	6.1	0.921	0.901	904	1.87	37	12.2	15.7	10.0
860310	0		20.9		3.4		268	10.9	0	0	906	1.62	50	8.1	23.2	10.0
860311	0		20.6		7.5		286	-6.8	0.728	0.694	905	1.72	50	9.5	21.7	3.1
860218	2		23.1		7.5		227	-14.8	0	0	953	1.42	37	5.9	17.9	8.1
860219	2		26.2		7.6		299	-1.3	0.898	0.885	953	1.88	37	10.0	15.1	6.6
860226	0		20.3		5.9		270	15.2	1	0.9917	948	1.69	37	18.8	19.3	10.0
860224	0		19.9		6.6		242	5.4	0	0	1005	1.58	37	9.6	19.9	15.0
860225	0		20.5		6.2		267	12.7	0.902	0.867	1005	1.75	37	15.8	20.0	8.5
					Limestone											
860317	2	0.28	24.8	0.83	5.5	1.97	316	2.7	0.633	0.615	901	1.90	37	13.8	25.2	24.0
860318	2		23.7		4.9	1.84	294	-0.5	0.963	0.956	852	1.69	37	23.7	26.8	14.5
860324	2		25.7		11.8	4.08	319	-0.2	0.951	0.931	900	1.91	37	12.1	15.2	12.0

*Based on Ca from sorbent, S from fuel. The fuel itself provides Ca/S = 0.05

Recycle of elutriated fines can significantly improve combustion efficiency for refractory fuels such as coke and char. Essentially two levels of recycle of cyclone catch were employed: zero and near-total.

Fluidizing velocity, so long as operation is maintained near stoichiometric, largely determines the system productivity in terms of rate of burning per unit bed area. Velocities above 2 m/s could not be practically used, due to increasing elutriation producing increasing freeboard burning with excessive freeboard temperatures. A lower limit on fluidizing velocity was set by the irreducible bed-cooling load presented by water-cooled portions of the combustor wall around the ports provided for insertion of in-bed heat exchange tubes. The rate of extraction of heat from the bed, $\dot{Q}_b$, to maintain a bed temperature in the range 850--1000 °C with operation near stoichiometric roughly obeys

$$\dot{Q}_b \propto \text{(combustion heat release)}$$
$$\propto \text{(fuel feed rate)}$$
$$\propto \text{(air feed rate)}$$

Thus, when as here, $\dot{Q}_b$ has a lower limit set by the apparatus, the fuel burning rate and air flow rate are thereby constrained. We would have preferred to conduct tests over a range of 0.5--3 m/s but practically could do no better than 1--2 m/s.

The effective expanded bed height is obtained from the vertical pressure distribution in the bed. Two levels were employed. Since higher bed heights give longer particle residence times and thus increase the time required to reach steady state, most runs were conducted at the lower height. It should be noted that the greater bed depth was obtained with underbed extraction of bed product, instead of by overflow. In this mode, the effective bed depth is maintained constant by extracting bed material at such a rate as to maintain constant

the pressure drop across the bed. In all the other runs, bed depth was maintained constant by letting bed product drain through an overflow orifice as indicated in Fig. 2.1.

5. Combustion performance

5.1 Oxygen utilization

Figure 5.1 shows the O_2 content of the exhaust gases as a function of the excess air level. Operation was conducted so that the exhaust O_2 level was always above 1 %. In cases of low combustion efficiency, the excess air level was sometimes negative despite quite high exhaust O_2 contents. The extreme case is a trial in which the exhaust O_2 content was 5.2 volume % but the excess air level was -10 %. The data are revealingly shown in another representation in Fig. 5.2 in which the exhaust O_2 flux is expressed as a fraction of the stoichiometric air requirement of the fuel.

5.2 Unburnt carbon levels and flows

As shown in Fig. 2.1, the system produces three streams of product solids:

[] the bed product, taken either as the overflow from an overflow orifice in the combustor wall or as material mechanically extracted, usually from the bottom, to maintain a constant bed depth. The first mode of operation was used here.

[] the cyclone product, a fraction 1 - r of the cyclone catch. The remaining fraction r is recycled, here by pneumatic conveying to the bottom of the bed

[] the baghouse product, the total catch in the baghouse. Baghouse material is normally not recycled in AFBC; in

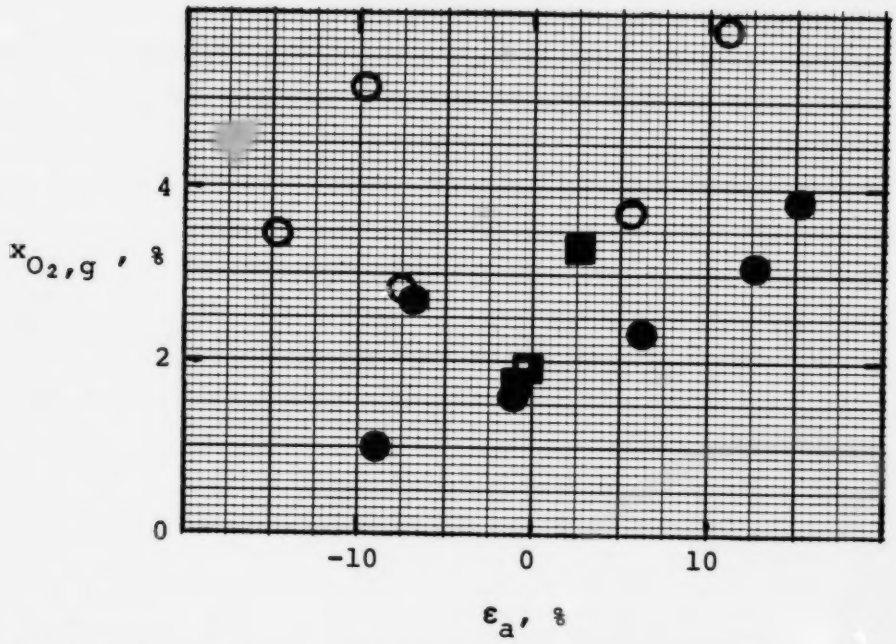

Fig. 5.1 Mole percent oxygen in the combustor exhaust gas vs the excess air level. Symbols: Table 4.2

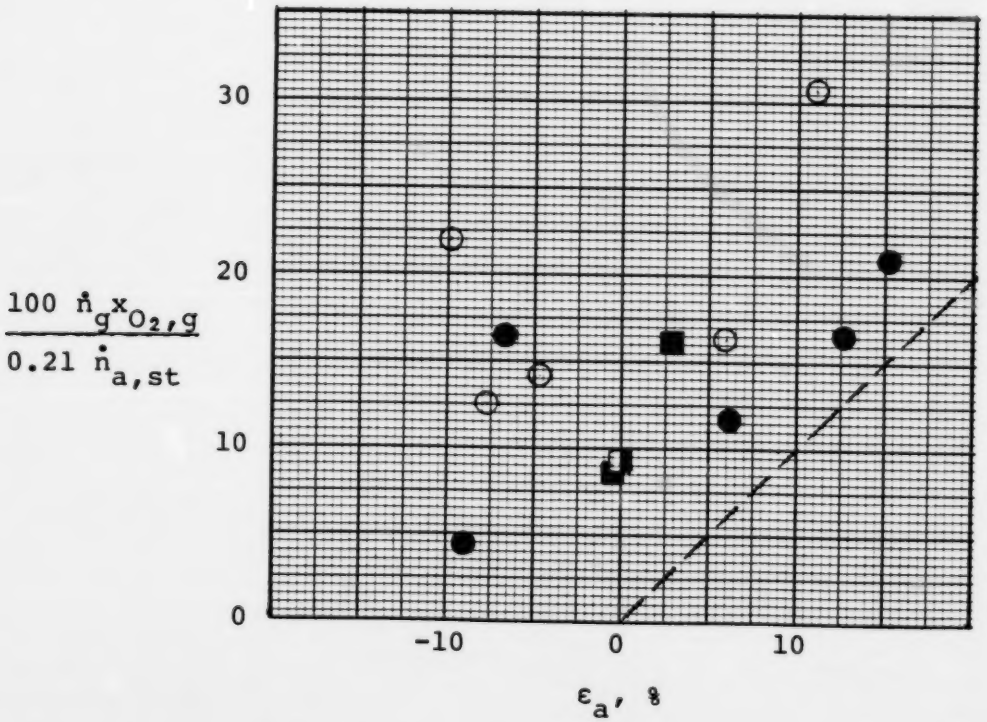

Fig. 5.2 Unreacted oxygen level vs excess air level. The former is the ratio of exhaust oxygen flux to the input flux theoretically required to burn the fuel. Equality, represented by the dashed line, exists in the case of perfect combustion. Symbols: Table 4.2

Table 4.2. Key to data symbols in the figures, except where otherwise shown in the figure caption

Symbol	Stone	r	Ca/S from stone
○	sand	0	0
●	sand	0.73--1	0
■	limestone	0.63--0.96	1.8--2.0
◨	limestone	0.95	4.1

circulating fluidized bed combustion (CFBC) it is sometimes partly recycled.

The major source of combustion inefficiency in FBC is the escape of unburnt carbon in the solid products. Figure 5.3 shows the carbon contents of the three product streams. As commonly happens, the baghouse and cyclone streams are typically much richer in unburnt carbon than the bed material. The major avenue of carbon loss tends to be by elutriation with the exhaust gases rather than simple convection out as part of the bed product.

The division of transport depends, of course, on the magnitude of the transporting streams as well as their composition. Figure 5.4 shows the flux ratio

$$\phi_{C,mf} = \frac{\text{carbon taken away in the m'th product stream}}{\text{carbon fed in fuel}}$$

for the three product streams. Except in some cases of very high recycle, the cyclone product is the major carbon carrier.

5.3 Carbon burnup efficiency

Combustion efficiency in FBC is usefully measured by the carbon burnup efficiency,

$$\eta_C = 1 - \frac{\text{loss of unburnt carbon}}{\text{carbon fed in fuel}} \quad .$$

It is commonly expressed as a percentage.

Figure 5.5 shows the carbon burnup efficiency as a function of bed temperature, T_b. A tendency for the efficiency to increase with T_b is apparent. The major effect, though, is that of recycle which quite dramatically improves performance. There is evidence that much of this improvement is due to greatly increased freeboard burning accompanying recycle. The recycle obviously results in substantial elevation of freeboard carbon

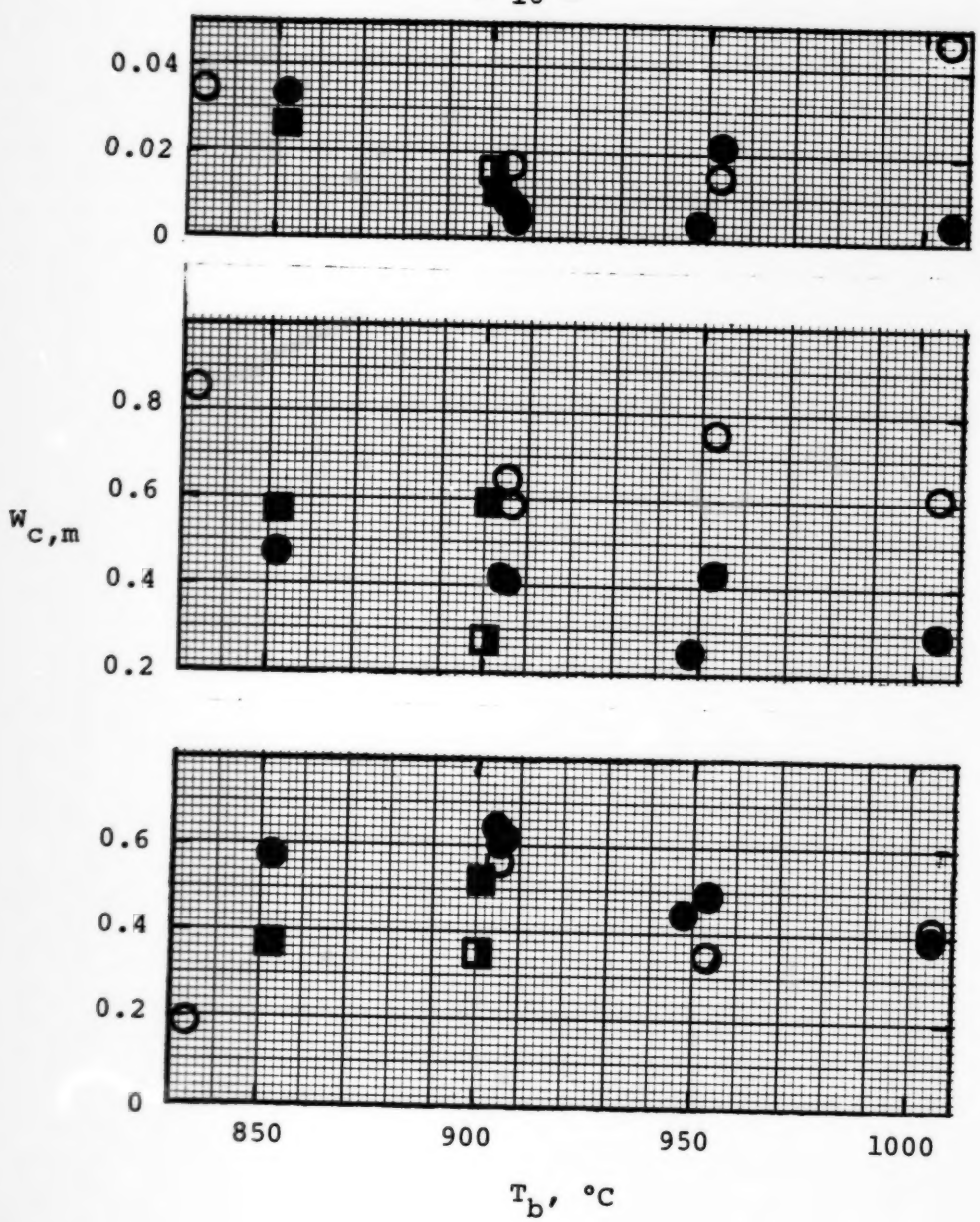

Fig. 5.3 Carbon content of the solid products as a function of bed temperature. Top, bed product; middle, cyclone product; bottom, baghouse product. Symbols: Table 4.2

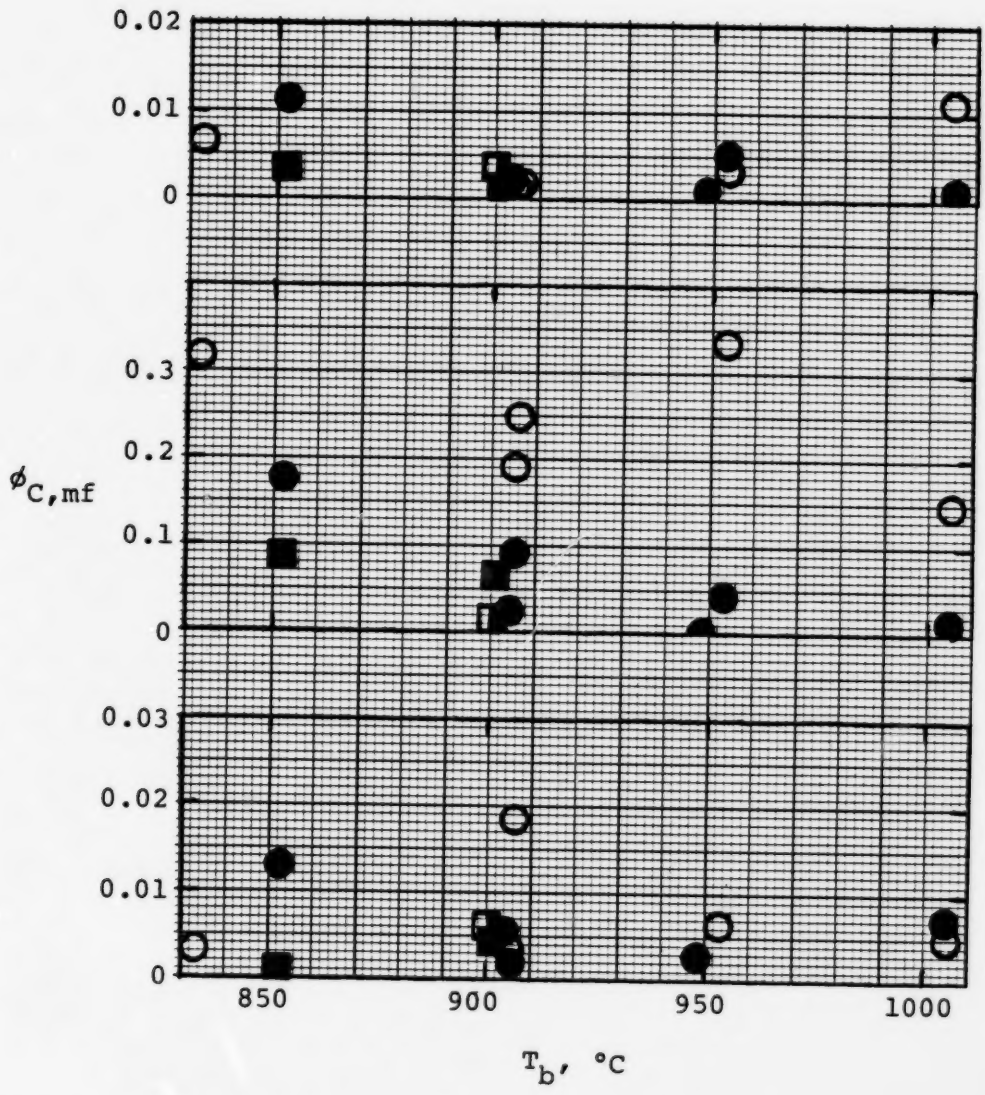

Fig. 5.4 Carbon flux carried by the solid products, expressed as a fraction of the input flux of fuel carbon, vs bed temperature. Top, bed product; middle, cyclone; bottom, baghouse. Symbols: Table 4.2

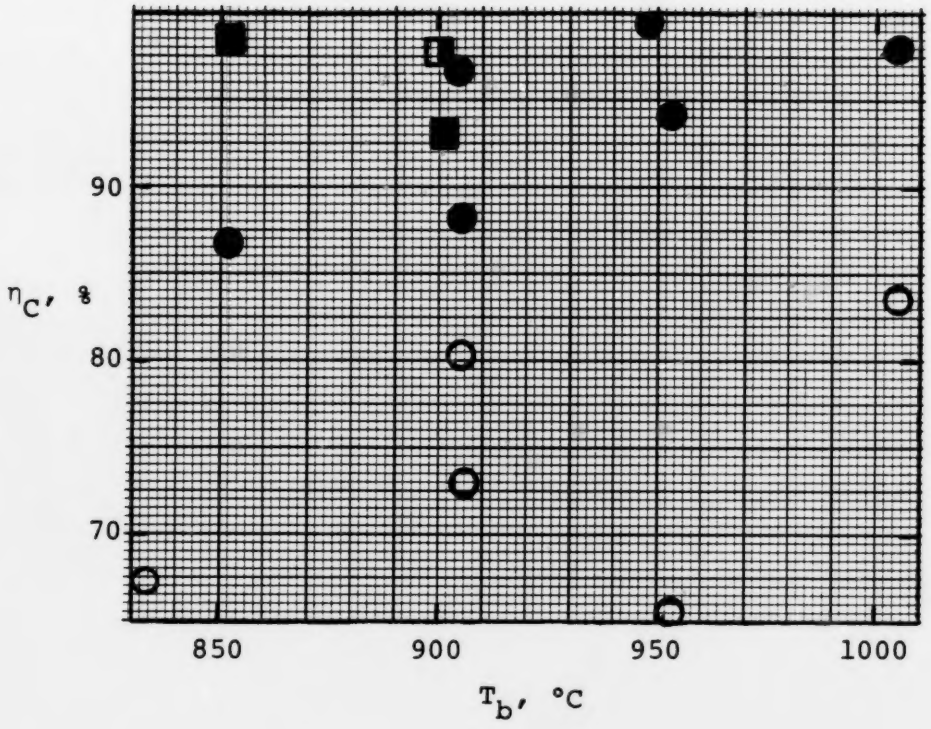

Fig. 5.5 Carbon combustion efficiency (percent of fuel carbon burnt) vs bed temperature. Symbols: Table 4.2

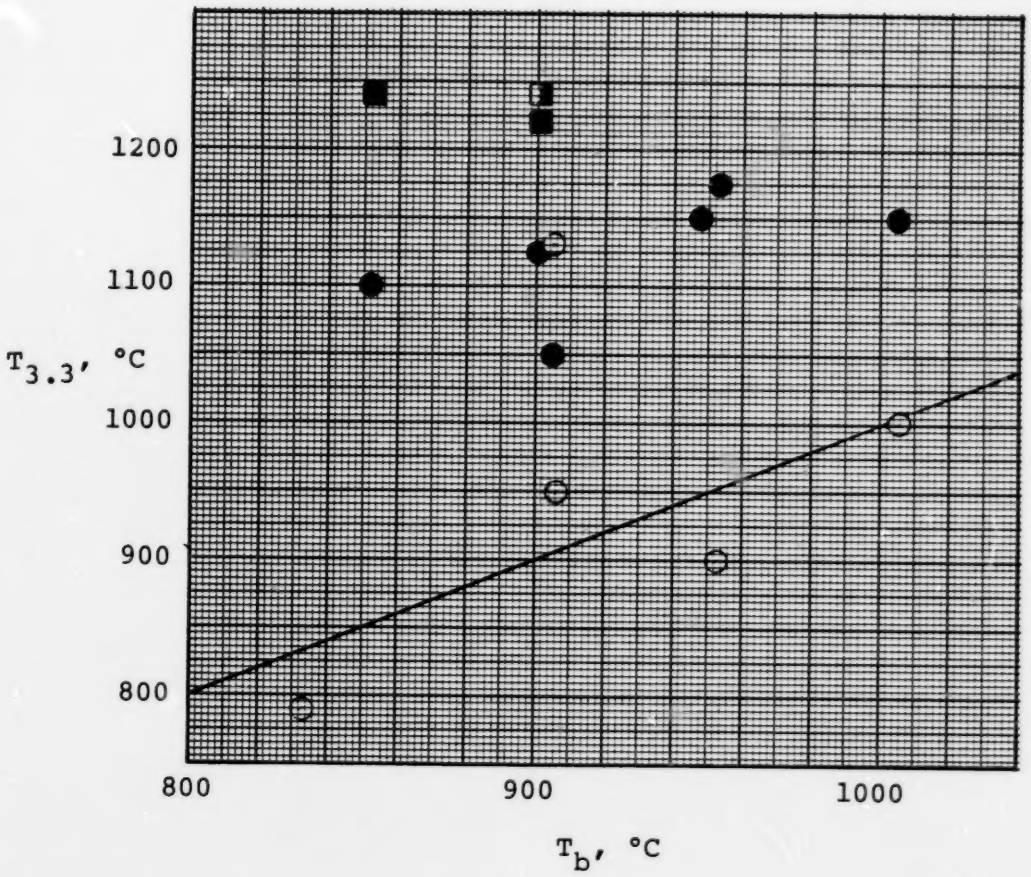

Fig. 5.6 Freeboard temperature 3.3 m above the distributor vs bed temperature. Symbols: Table 4.2. Straight line: $T_{3.3} = T_b$

(char particle) concentrations, fueling reaction there. Figure 5.6 shows the freeboard temperature 3.3 m above the distributor, not far from the exit. With one exception, these freeboard temperatures in the absence of recycle are within 50 °C of the bed temperatures. With recycle, they jump by 150--390 °C. An interesting result is that the combustion efficiency appears to depend strongly on the freeboard temperature, Fig. 5.7. Since freeboard temperature is a dependent variable, recycle must still be regarded as the basic driving factor. However, the effect of recycle is clearly complex. The primary effect of recycle, always present, is to improve combustion by increasing the residence time of the fine char particles, difficult to burn because they are so quickly elutriated. The complication here is the strong added effect of the elevation in freeboard temperature.

5.4 Correlation of carbon loss with operating variables

The data on carbon loss have been statistically analyzed according to models shown to be useful by our earlier studies of other fuels, including Syncrude coke. The basic model is

$$y = \Sigma_i a_i x_i \quad . \tag{5.1}$$

The full set of influential independent variables x_i normally includes

$$x_1 = \ln v, \quad x_2 = \ln \hat{D}_{ps}, \quad x_3 = \ln \phi_a, \quad x_4 = r, \quad x_5 = 1/T_b \quad .$$

The dependent variable of interest is either

$$y = \ln(\dot{m}_{C,o}/\dot{m}_{C,f}) \text{ or } \ln (\dot{m}_{C,b}/\dot{m}_{C,f})$$

where $\dot{m}_{C,o}/\dot{m}_{C,f}$ is the combustion inefficiency due to overhead carbon loss (that in the cyclone and baghouse products), and

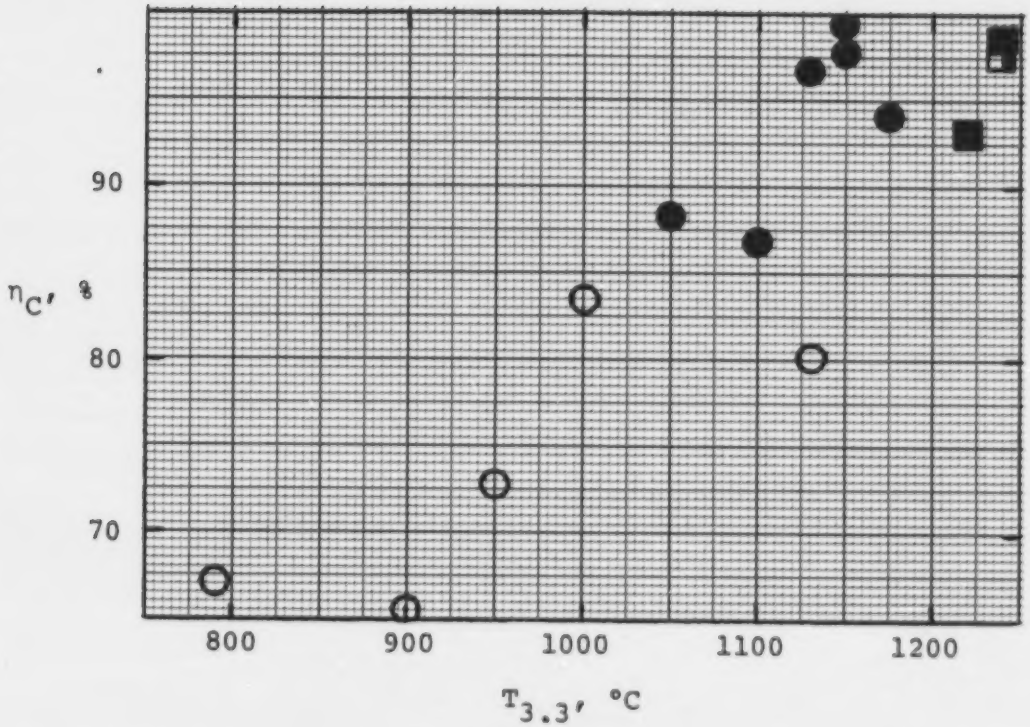

Fig. 5.7 Carbon combustion efficiency vs freeboard temperature 3.3 m above the distributor. Symbols: Table 4.2

$\dot{m}_{C,b}/\dot{m}_{C,f}$ is the inefficiency due to loss in the bed product. The overall <u>efficiency</u> η_C is related to these by

$$\eta_C = 1 - \dot{m}_{C,o}/\dot{m}_{C,f} - \dot{m}_{C,b}/\dot{m}_{C,f} \qquad (5.2)$$

In power-law form, (5.1) gives with the variables mentioned

$$\dot{m}_{C,n}/\dot{m}_{C,f} = C\, v^{a_1}\, \hat{D}_{ps}^{a_1}\, \phi_a^{a_3}\, e^{a_4 r}\, e^{a_5/T_b} \quad , \qquad (5.3)$$

where n denotes subscripts o or b and $C = \ln^{-1} a_o$. The coefficients a_i are, of course, different in the two cases (overhead product loss and bed product loss).

Table 5.1 shows results of multiple linear regression analysis for the overhead carbon loss according to this model. The full model as specified above was first fitted. Partial models retaining only the strongest effects were then considered. In the first, the variables v and $\hat{D}_{ps}$ were omitted (effectively setting $a_1 = a_2 = 0$), and in the second ϕ_a was omitted too. Since it is possible that limestone and sand affect the combustion process in more complex ways than through just particle diameter, the results for sand beds were also analyzed separately. Finally, examination of residuals indicated that one trial, 860226, with atypical results was unduly influencing the statistical estimations. The carbon burnup, $\dot{m}_{C,o}/\dot{m}_{C,f} = 0.0029$ as measured, was so nearly complete in this trial as to be exceptionally susceptible to errors of, for example, chemical analysis. Practically, and on an absolute basis, values of $\dot{m}_{C,o}/\dot{m}_{C,f}$ of, say, 0.0029 and 0.0015 are not very different; both are very small. Our regression analysis, however, takes the logarithm of $\dot{m}_{C,o}/\dot{m}_{C,f}$ and thus focusses on relative magnitudes; in these terms 0.0029 and 0.0015 are far apart, one being twice the other. The regression analysis was therefore repeated omitting trial 860226, with notable improvement, Table 5.1. Further comparisons can be seen in Figs. 5.8 and 5.9 where

Table 5.1. Statistical fitting* of model for overhead carbon loss,

$$y = a_o + a_1x_1 + a_2x_2 + a_3x_3 + a_4x_4 + a_5x_5$$

$y = \ln(\dot{m}_{C,o}/\dot{m}_{C,f})$ $x_1 = \ln v$ $x_2 = \ln \hat{D}_{ps}$ $x_3 = \ln \phi_a$

$a_o = \ln C$ $x_4 = r$ $x_5 = 1/T_b$

Stone, trials	a_o / s_o	C	a_1 / s_2	a_2 / s_2	a_3 / s_3	a_4 / s_4	a_5 / s_5	s_y	R^2
Sand & limestone, all trials	-8.15	0.00029	2.31	-2.41	-5.84	-2.49	5370		
	7.44		2.21	1.90	2.84	0.64	7743	0.75	0.84
	-1.12	0.326	0	0	-5.61	-2.29	465		
	5.36		--	--	2.78	0.51	6432	0.74	0.80
	-6.26	0.0019	0	0	0	-2.72	5937		
	5.34		--	--	--	0.53	6333	0.84	0.71
Sand, all trials	-7.23	0.00073	1.73	0	-5.88	-2.26	5950		
	7.21		2.34	--	2.96	0.68	8094	0.77	0.83
	-4.38	0.0125	0	0	-5.54	-1.99	3363		
	5.90		--	--	2.83	0.55	7065	0.75	0.82
	-9.84	0.000053	0	0	0	-2.37	10154		
	6.05		--	--	--	0.60	7170	0.86	0.71
Sand & limestone, all trials except 860226	-7.07	0.00085	0.96	-2.97	-3.11	-2.00	4456		
	5.30		1.63	1.36	2.21	0.48	5511	0.53	0.88
	-0.97	0.38	0	0	-3.61	-2.13	591		
	4.39		--	--	2.41	0.42	5264	0.61	0.80
	-3.87	0.021	0	0	0	-2.35	3028		
	4.17		--	--	--	0.42	4954	0.65	0.75
Sand, all trials except 860226	-5.89	0.0028	0.20	0	-2.97	-1.71	5136		
	3.71		1.25	--	1.67	0.37	4153	0.40	0.91
	-5.57	0.0038	0	0	-2.90	-1.68	4857		
	2.87		--	--	1.47	0.28	3439	0.36	0.91
	-0.22	0.00027	0	0	0	-1.82	8146		
	3.00		--	--	--	0.32	3567	0.43	0.85

* s_i = standard error of estimate of a_i

s_y = standard error of prediction of y

R^2 = coefficient of multiple correlation

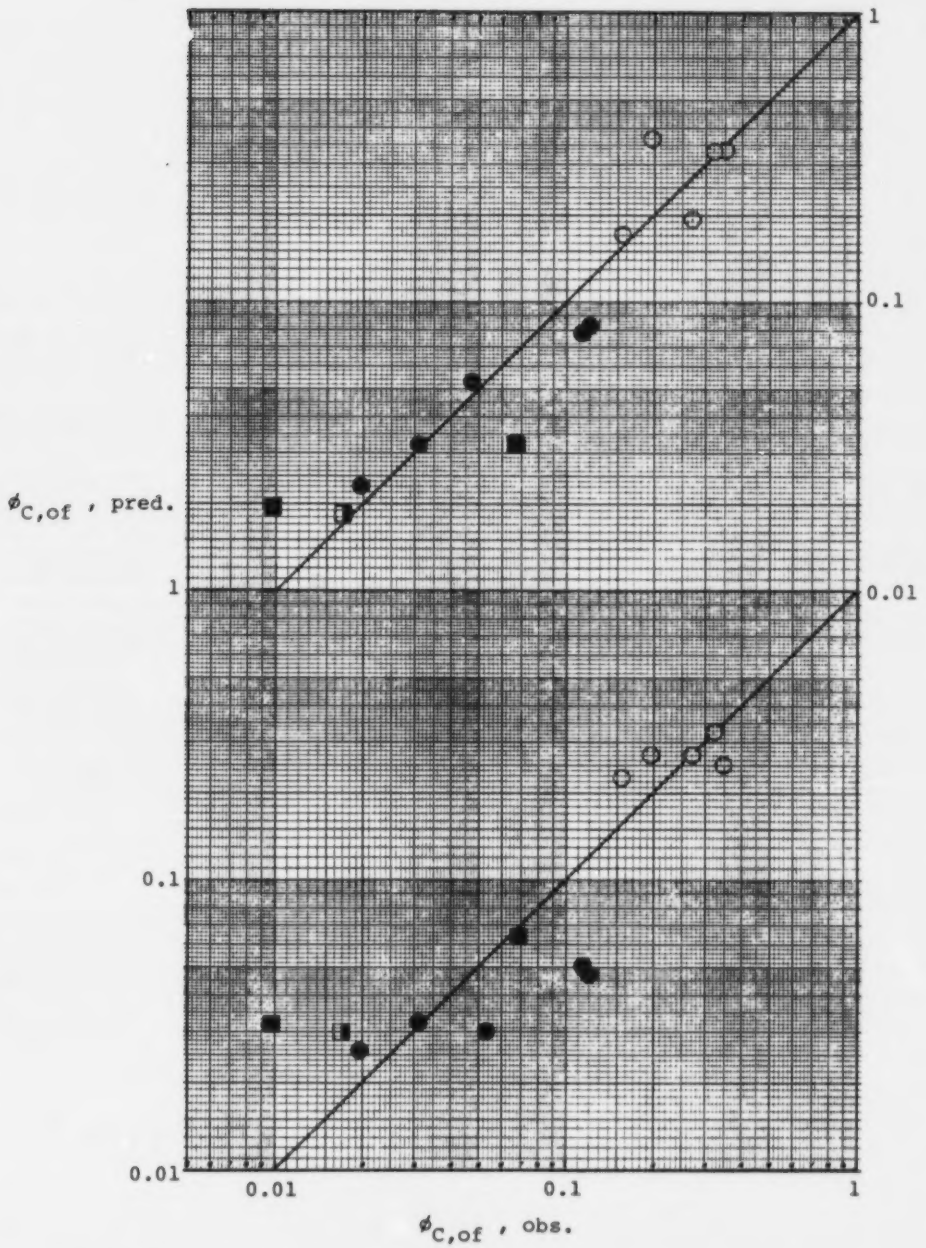

Fig. 5.8 Predicted overhead carbon loss vs that measured, both normalized on fuel carbon fed, for all trials except 860226. Predictions from models in Table 5.1: top, independent variable set {v, D_{ps}, ϕ_a, r, T_b}; bottom {r, T_b}. Symbols: Table 4.2

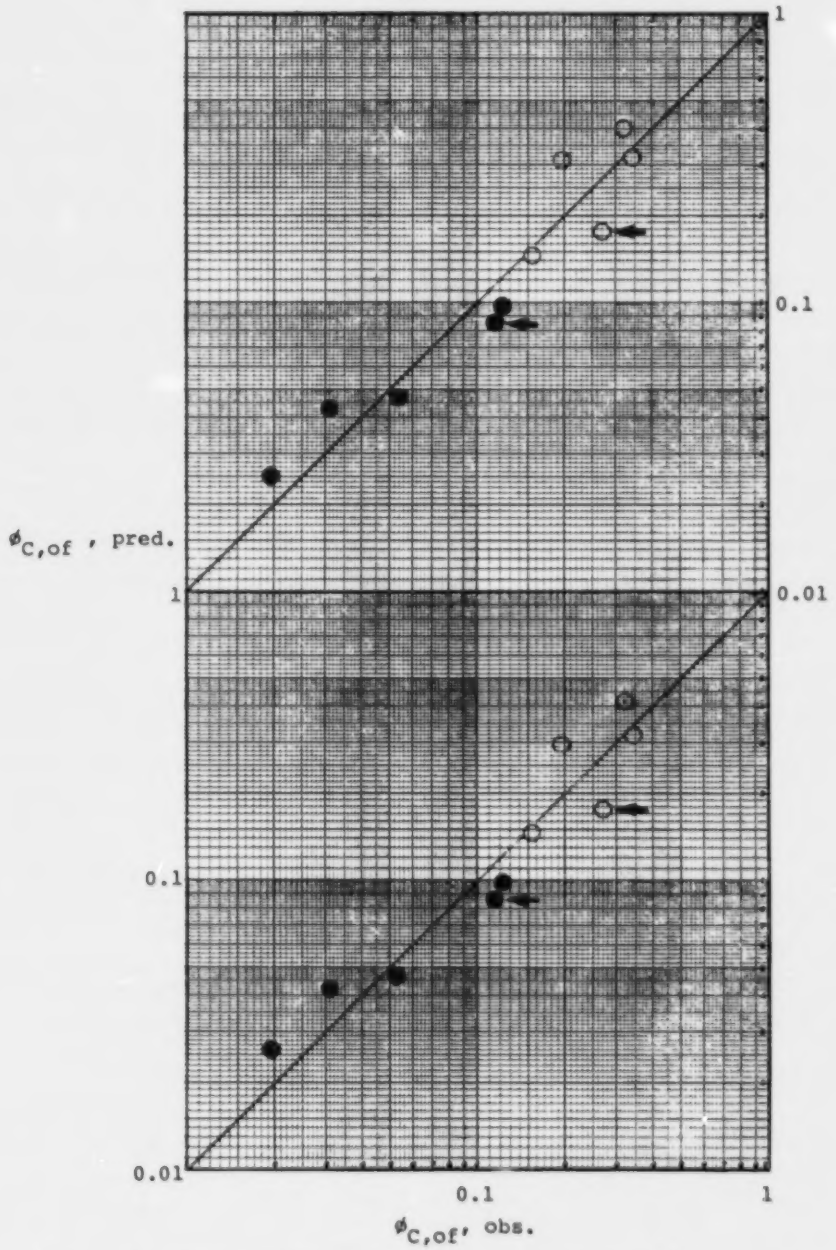

Fig. 5.9 Predicted overhead carbon loss vs that measured, both normalized on fuel carbon bed, for all trials with sand beds except 860226. Predictions from the models in Table 5.2: top, independent variable set (v, ϕ_a, r, T_b); bottom, (ϕ_a, r, T_b). Symbols: Table 4.2

overhead carbon loss predicted by several forms of the statistical model is compared with the observed loss.

Examination of Fig. 5.9 shows that the predicted overhead carbon losses in the two runs at increased bed height (50 cm expanded height compared to 38 cm in the others) are both low; these are, in fact, the extreme cases of under-prediction. The model was therefore extended to include $x_6 = \ln H$ and the statistical analysis was repeated. Table 5.2 shows the results of interest for the sand beds. The correlation is significantly improved, as may be seen also in Fig. 5.10. The apparent effect of bed height is substantial, with the overhead carbon loss varying as $H^{1.8}$. The fact that increasing bed height increases the loss is unexpected and raises questions as to the nature of the responsible mechanism. The exponent of the fluidizing velocity is diminished from $a_1 = 2$, Table 5.1, to $a_1 = 0$, Table 5.2. This marked change suggests a weakness in the experimental design which, as noted earlier, was only partly controllable.

Statistical analysis of the bed carbon loss $\dot{m}_{C,b}/\dot{m}_{C,f}$, usually much smaller than $\dot{m}_{C,o}/\dot{m}_{C,f}$, Fig. 5.4, was rather inconclusive because of relatively high scatter. The strongest variables affecting $\dot{m}_{C,b}/\dot{m}_{C,f}$, Table 5.2, are apparently the fluidizing velocity v and the expanded bed depth H; the regression analysis upon these alone gives

$$\dot{m}_{C,b}/\dot{m}_{C,f} = 0.0055\ v^{-1.82}\ H^{-0.37}$$

The indication that bed depth has a positive exponent for overhead carbon loss but a negative one for bed carbon loss is significant; a negative correlation is indeed to be expected.

The bed carbon loss, Figs. 5.10 and 5.11, was never over 1/3 the overhead loss. In only three of the fourteen runs was it over 1/10 the overhead loss. In the runs with no recycle, it was around 1/100 the overhead loss.

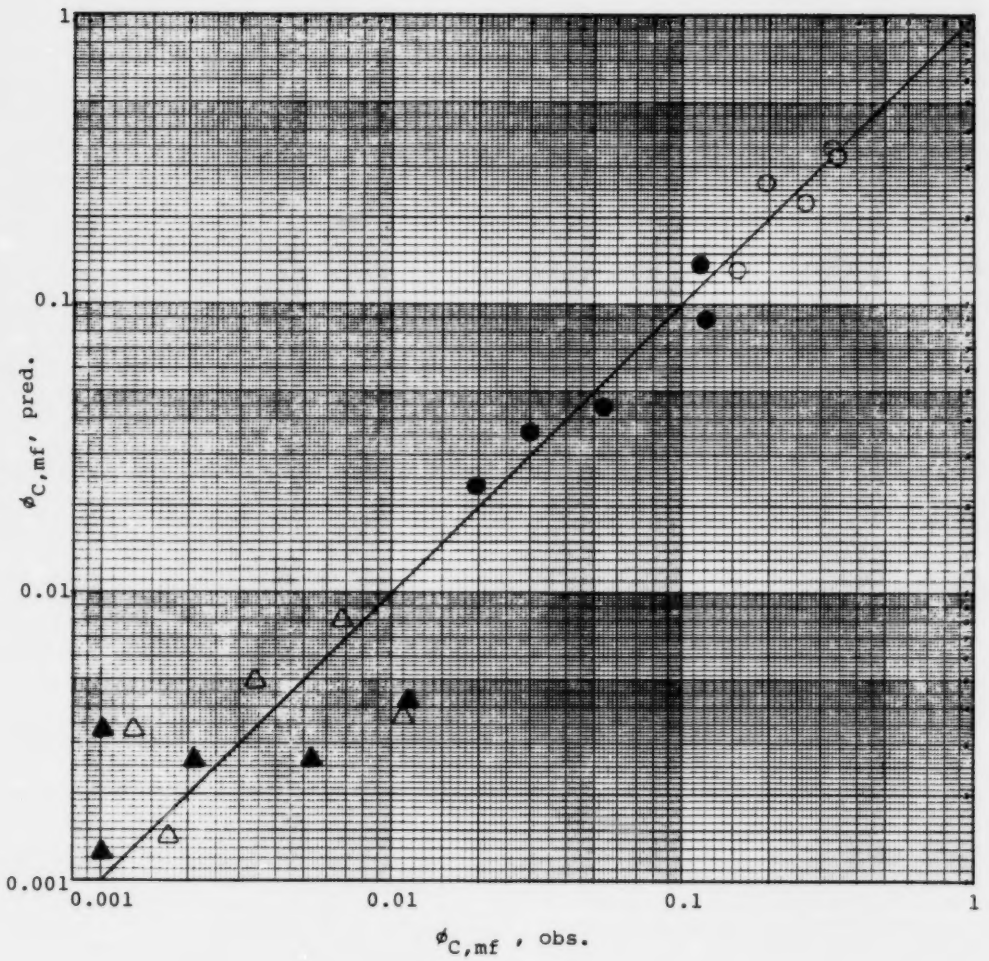

Fig. 5.10 Predicted carbon loss vs that measured, both normalized on fuel carbon fed, for all trials with sandbeds except 860226. Predictions from the models in Table 5.2 for overhead carbon loss (○, ●), independent variable set {ϕ_a, r, T_b, H}, and bed carbon loss (△, ▲), independent variable set {v, H}. Cyclone recycle fraction r: ○△, 0; ● ▲, 0.73--0.92

Table 5.2. Statistical fitting* of model for carbon loss, including effect of bed height.

$$y = a_o + a_1x_1 + a_2x_2 + a_3x_3 + a_4x_4 + a_5x_5 + a_6x_6 ,$$

$y = \ln(\dot{m}_{C,o}/\dot{m}_{C,f})$ for overhead carbon loss

$y = \ln(\dot{m}_{C,b}/\dot{m}_{C,f})$ for bed carbon loss

$a_o = \ln C$ $\quad x_1 = \ln v$ $\quad x_2 = \ln \hat{D}_{ps}$ $\quad x_3 = \ln \phi_a$

$x_4 = r$ $\quad x_5 = 1/T_b$ $\quad x_6 = \ln H$

	a_o	C	a_1	a_2	a_3	a_4	a_5	a_6		
	s_o		s_2	s_2	s_3	s_4	s_5	s_6	s_y	R^2
Overhead carbon loss, sand beds, 860226	-1.79	0.17	-0.35	0	-3.72	-1.54	2545	1.89		
	3.39		0.98	--	1.31	0.29	3370	0.87	0.30	0.959
omitted	-2.48	0.084	0	0	-3.80	-1.60	3119	1.80		
	2.52		--	--	1.17	0.21	2693	0.76	0.27	0.958
Bed carbon loss, sand beds, 860226	-2.85	0.06	-2.38	1.57	-1.12	0.15	1868	-0.48		
	10.27		3.25	2.88	4.29	0.98	10667	0.65	1.02	0.27
omitted	-5.20	0.0055	-1.82	0	0	0	0	-0.37		
	0.99		1.61	--	--	--	--	0.45	0.82	0.21

* s_i = standard error of estimate of a_i

s_y = standard error of prediction of y

R^2 = coefficient of multiple correlation

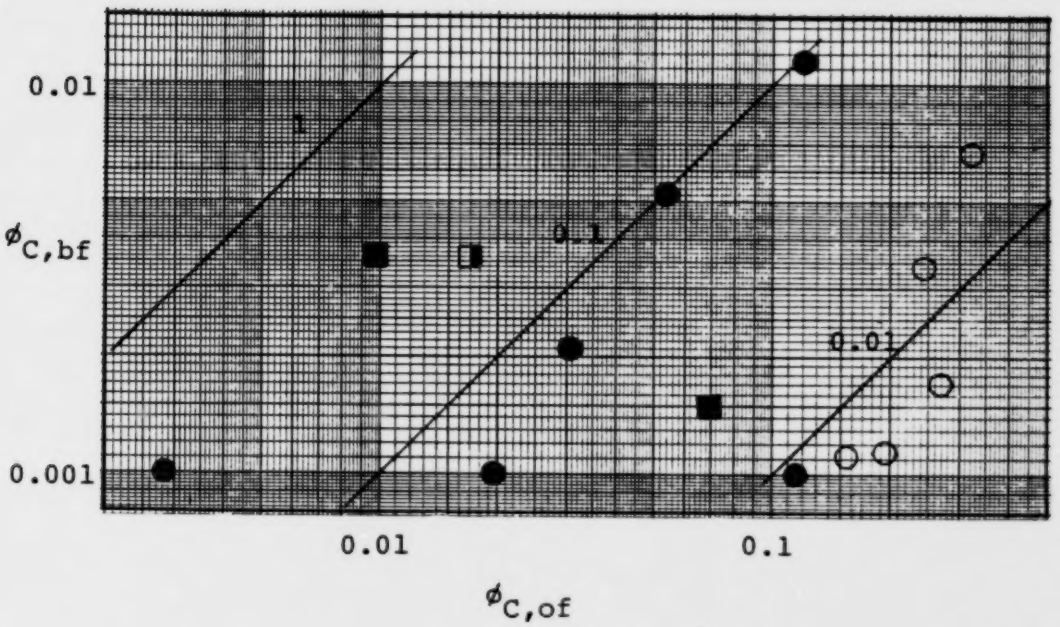

Fig. 5.11 Carbon flux in bed product vs carbon flux in overhead products, both normalized on fuel carbon fed. Symbols: see Table 4.2. Straight lines: $\phi_{C,bf} = a\ \phi_{C,of}$ with a = {1, 0.1, 0.01}

Comparisons with findings from past work on other fuels, are given in the Discussion (Sect. 9).

5.5 Carbon balance

Figure 5.12 shows the results of the overall carbon balance, comparing the flux of carbon leaving the combustor with the carbon fed. The balance is satisfactory (within 6 % of equality) in all runs except for one sand run with recycle (860311) in which the carbon leaving was measured as 89 % of that fed and the one limestone run (860324) with the high Ca/S ratio of 4.1 in which it was only 82 %. The unusual discrepancy in the first case, Table 4.1, can be ascribed to inadequate operating time, only 3.1 h under continuous feed, less than half the next smallest value. In the second case, no plausible explanation is readily evident.

6. Sulphur capture

6.1 Sulphur capture efficiency

Gas analysis and mass balances give the fraction of fuel sulphur converted to gaseous products, basically SO_2, and emitted with the stack gases. The remaining sulphur, fixed in the solid products, is said to be "captured", meaning that it did not escape as SO_2. The capture efficiency, η_S, is given by

$$\eta_S = \phi_{S,pf} = 1 - \phi_{S,gf} \quad . \tag{6.1}$$

It is commonly expressed as a percentage. The flux ratio

$$\phi_{S,pf} = \dot{m}_{S,p} / \dot{m}_{S,f}$$

is determined experimentally from the solids analyses and flowrates while

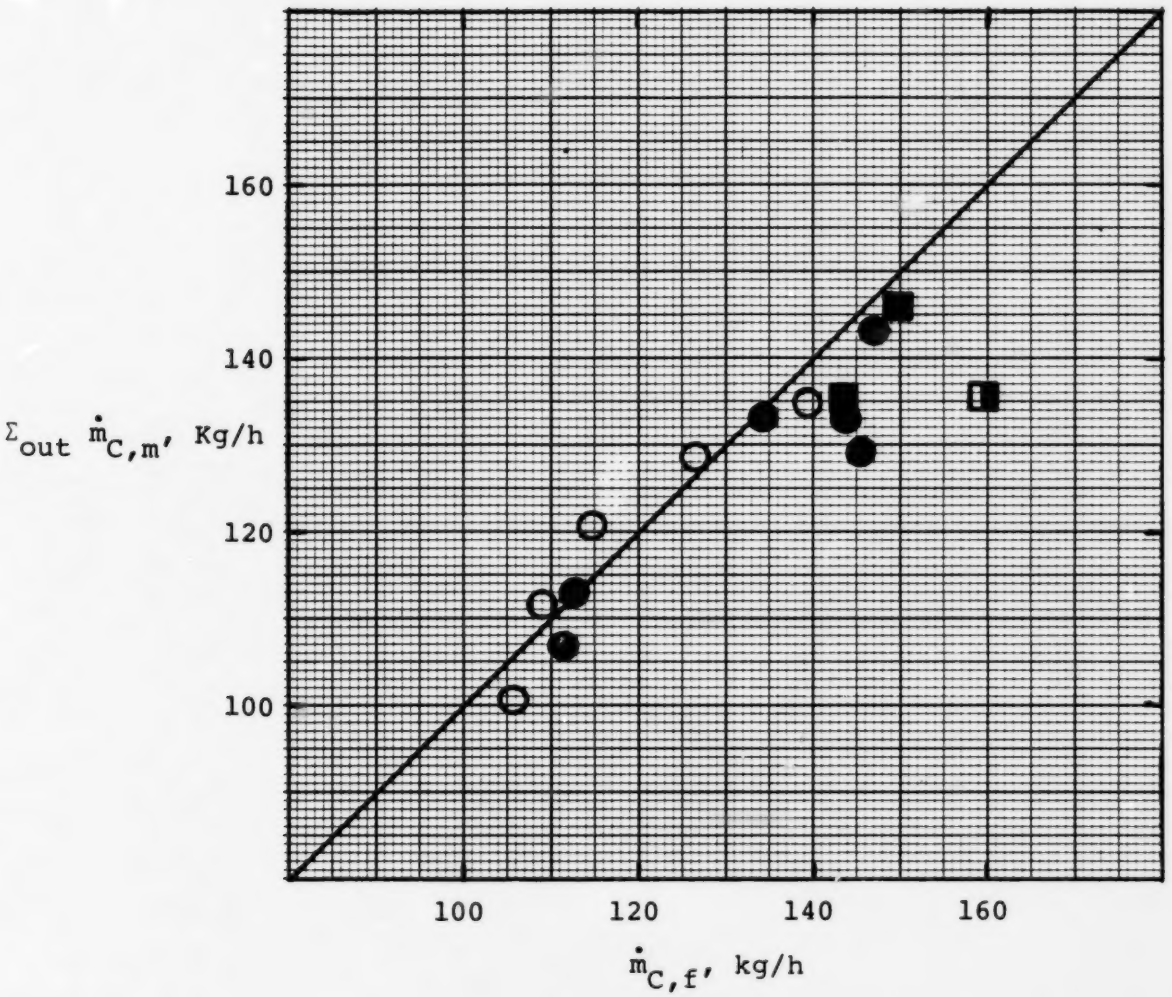

Fig. 5.12 Carbon balances: carbon out vs carbon in. Symbols: 4.2

$$\phi_{S,gf} = \dot{m}_{S,g}/\dot{m}_{S,f}$$

is determined from the gas analysis and flow. Because of measurement errors and departures from true steady-state operation, values of η_S found by these two methods normally do not agree exactly and sometimes differ significantly.

The ash of the coke fuel, Table 3.1, contains enough Ca to convert 5.2 % of the fuel sulphur to $CaSO_4$ if fully utilized. In other words, the fuel itself provides a Ca/S mole ratio of 0.052. If the Mg, Ba, Sr, Na and K were also sulphated, the total fixation would be 6.2 % of the sulphur.

Figure 6.1 shows as a function of bed temperature the observed sulphur capture efficiency based on gas analysis. The capture in the trials with limestone, 40--60 %, is unusually low for Ca/S mole ratios of 2--4. On the other hand, the capture in nearly all trials with sand beds is much higher than the low level, at most 6.2 %, that can there be accounted for by fixation in mineral sulphates.

In seeking explanations of these observations, the first question arising obviously concerns the quality of the sulphur balances. Good balances will support the validity of the observations for which physico-chemical explanations must then be found. Figure 6.2 shows that the balances were satisfactory in all but three trials: one (860212) with sand and no recycle, one (860226) with sand and recycle, and one (860318) with limestone and recycle. In all three cases, solids analysis indicated less sulphur capture than did gas analysis. On the whole, however, the validity of the data is upheld.

To what, then, can the evidently real high sulphur fixation in the trials with sand beds be attributed? The only obvious possibility is that the sulphur, almost entirely organic in original form, Table 3.1, remains bound up with the unburnt

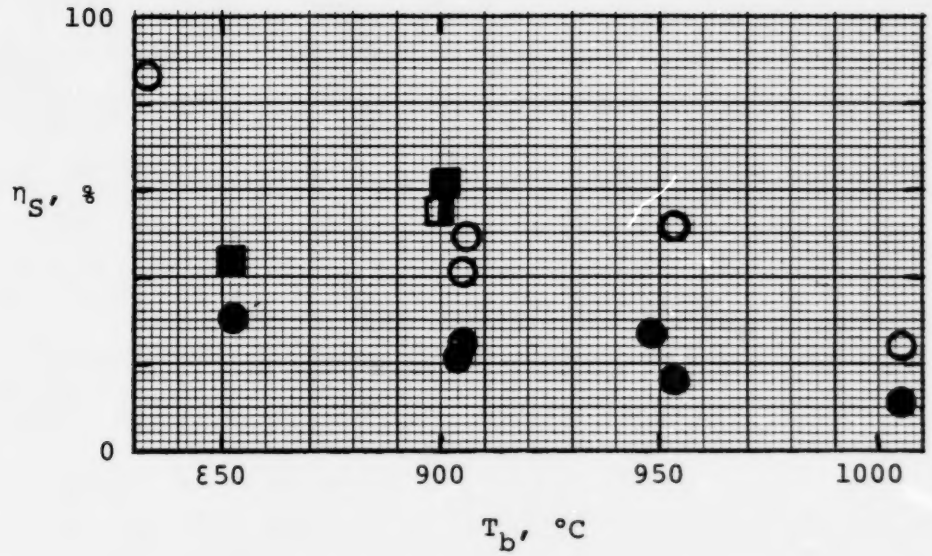

Fig. 6.1 Sulphur capture, as indicated by gas analysis, vs bed temperature. Symbols: Table 4.2

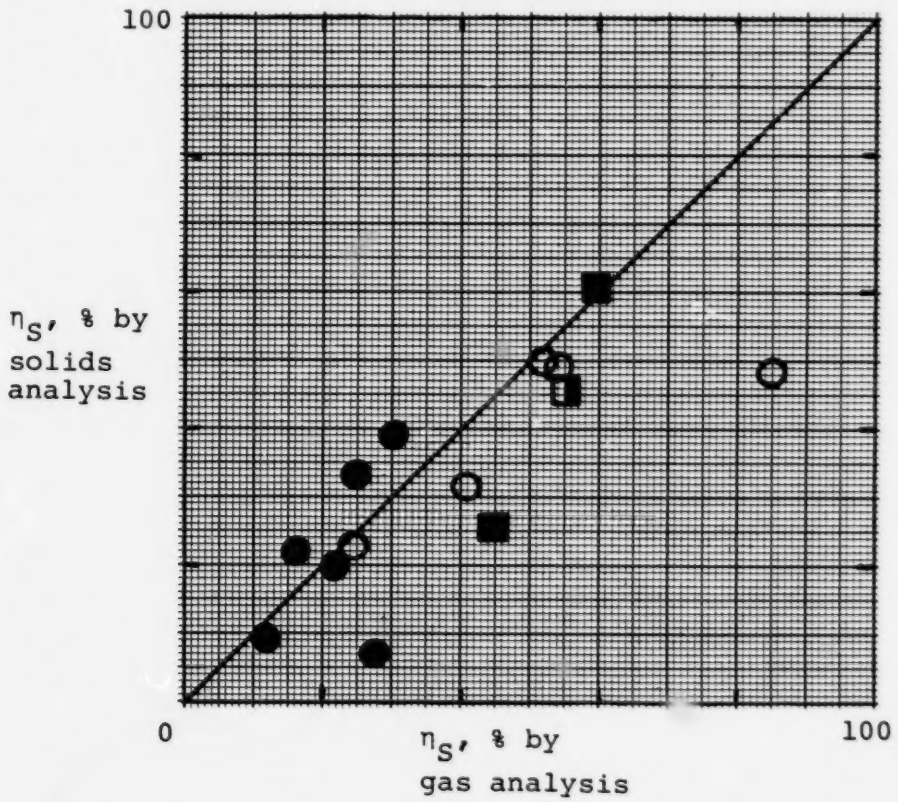

Fig. 6.2 Sulphur balances: sulphur capture as indicated by analysis of solid products vs that indicated by exhaust gas analysis. Symbols: Table 4.2

carbon. If so, then a correlation can be expected between the flux ratios

$\phi_{S,pf}$ = fraction of the fuel sulphur accounted for by the solid product streams (equals the sulphur capture efficiency),

$\phi_{C,pf}$ = fraction of the fuel carbon accounted for by the solid product streams (equals the carbon combustion inefficiency)

Figure 6.3 shows the suggested graphs and strongly supports this explanation. The sulphur "capture" beyond the base level set by the minerals in the ash, principally the calcium, evidently occurs in simple proportion to the flux of unburnt carbon. Based on the solids analysis, for the trials with sand and no recycle

$$\phi_{S,pf} = Ca/S + 1.3\ \phi_{C,pf} \qquad (6.2)$$

With recycle of most or all of the cyclone catch,

$$\phi_{S,pf} = Ca/S + 2.7\ \phi_{C,pf} \cdot \qquad (6.3)$$

Equation (6.2) indicates a 30 % enrichment in sulphur relative to carbon and (6.3) a 170 % enrichment. This seems qualitatively consistent; the small char particles primarily responsible for combustion inefficiency are enriched in sulphur and when they are retained longer and burnt down further by recycle, the residue is further enriched.

The results based on gas analysis, Fig. 6.3, show more scatter and less differentiation; with or without recycle, the data from the trials with sand beds are fitted about equally well by

$$\phi_{S,pf} = Ca/S + 1.8\ \phi_{C,pf} \cdot \qquad (6.4)$$

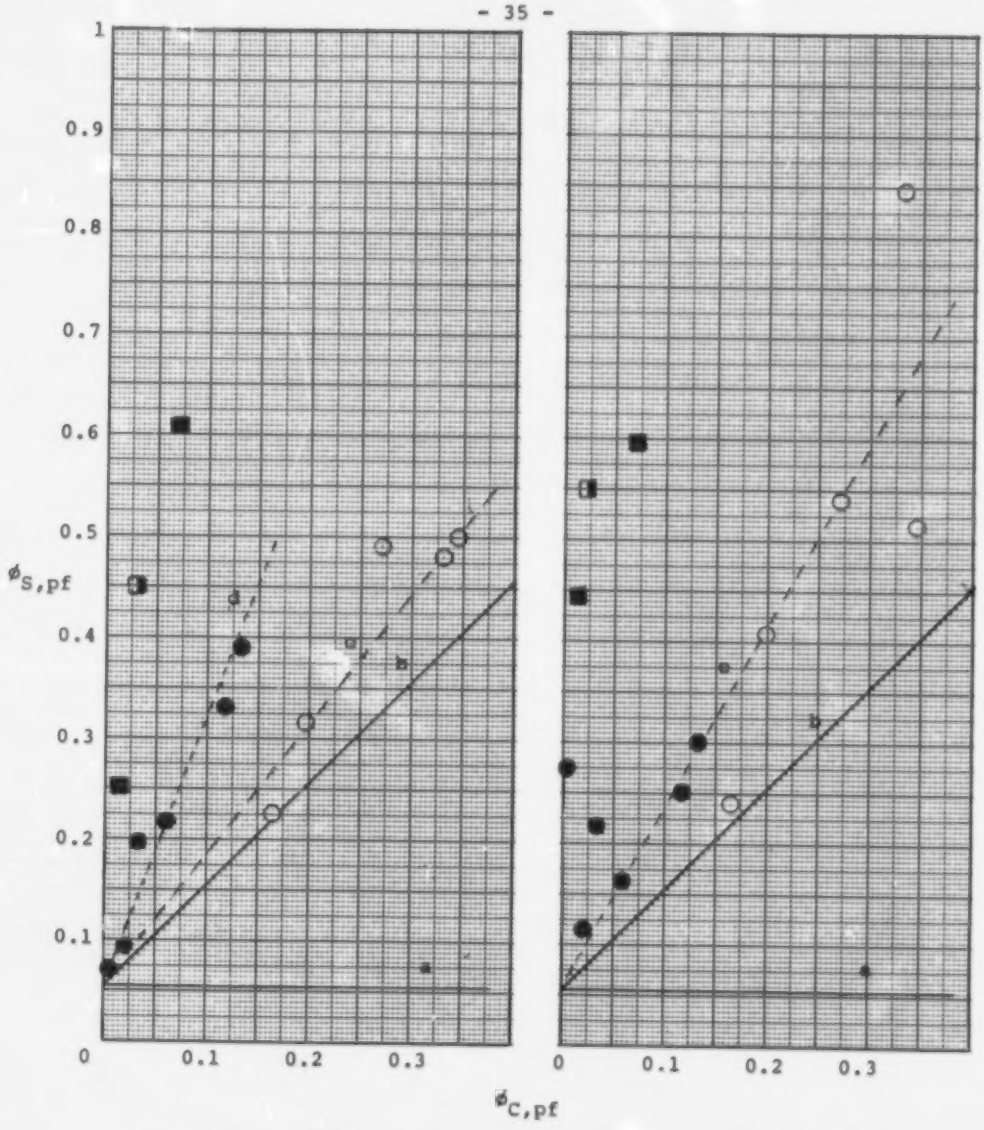

Fig. 6.3 Sulphur leaving in solid products as a fraction of fuel sulphur fed vs carbon leaving in solid products as a fraction of fuel carbon fed. Left, sulphur based on analysis of solid products; right, sulphur based on gas analysis. Curves: $\phi_{S,pf} = Ca/S + k, \phi_{C,pf}$ with a, k = 0; b, k = 1; c, k = 1.3; d, k = 2.7; e, k = 1.8. Symbols: Table 4.2

Based on consistency in trend, however, the results of the solids analysis look more convincing and should, we feel, be accepted as most significant.

6.2 Sulphur levels and division of fluxes

The above examination has demonstrated the overall features of the fate of sulphur in the burning of the petroleum coke. It remains to see how the captured sulphur is divided between the three product streams. Figure 6.4 shows as a function of bed temperature the sulphur contents of the streams. In the runs with limestone, the prominence of $CaSO_4$ in the bed product is clear; the levels in the cyclone and baghouse products, however, are very similar to those in the runs with sand. Typical levels in the cyclone product are 3--4 %, and in the baghouse product they are 4--6 %.

The results on sulphur transport, Fig. 6.5, show greater spread than those on sulphur content. In view of the observations on overall sulphur fixation, Sect. 6.1, the parallel between sulphur transport and carbon transport by the cyclone product seen in Figs. 6.5 and 5.4 is truly striking. Similarity of the results for bed and baghouse streams is much weaker.

Figure 6.6 shows how the total sulphur flux in the solid products is divided among the three streams. As usual, there is a pronounced effect of recycle. Recycle diminishes the portion of sulphur carried by the cyclone product and increases that in the bed product. The correlation with carbon flow is as expected; recycle increases bed levels of carbon and nearly proportionally increases the flux in the bed product. At the same time, recycle more strongly diminishes the loss of carbon in the cyclone product.

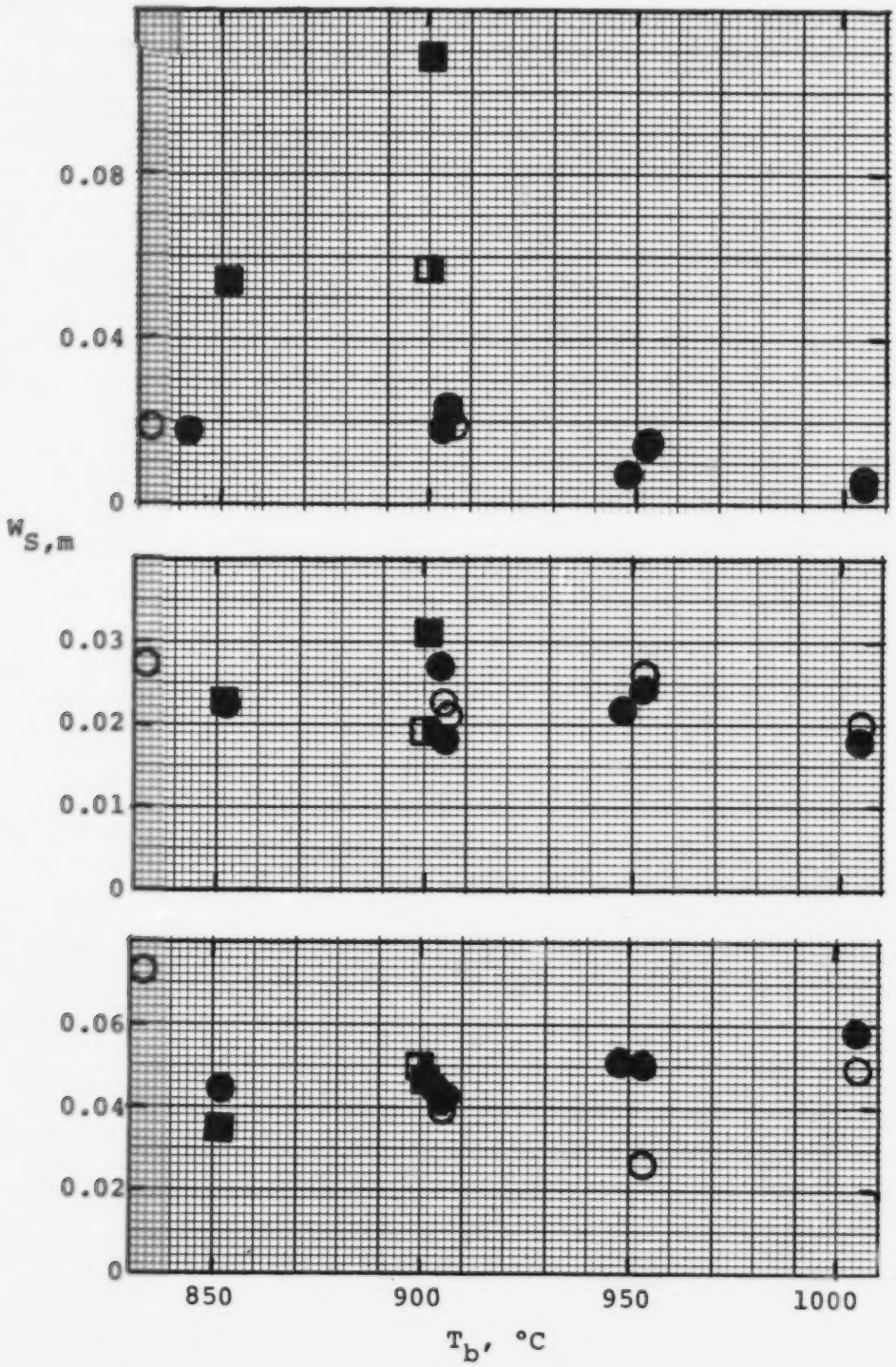

Fig. 6.4 Sulphur content of solid products vs bed temperature. Top, bed product; middle, cyclone; bottom, baghouse. Symbols: Table 4.2

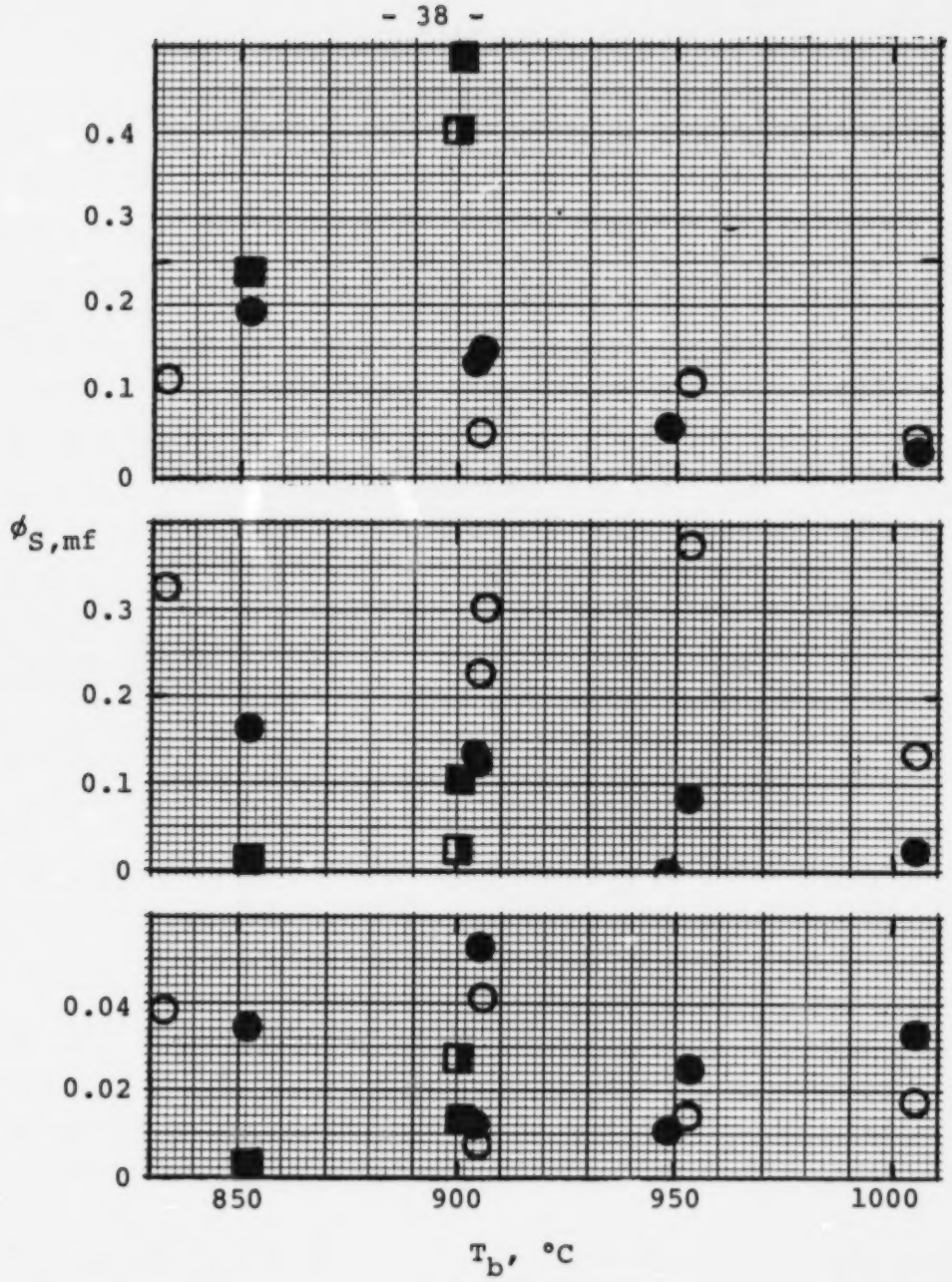

Fig. 6.5 Sulphur flux carried by the solid products, expressed as a fraction of fuel sulphur fed, vs bed temperature. Top, bed product; middle, cyclone; bottom, baghouse. Symbols: Table 4.2

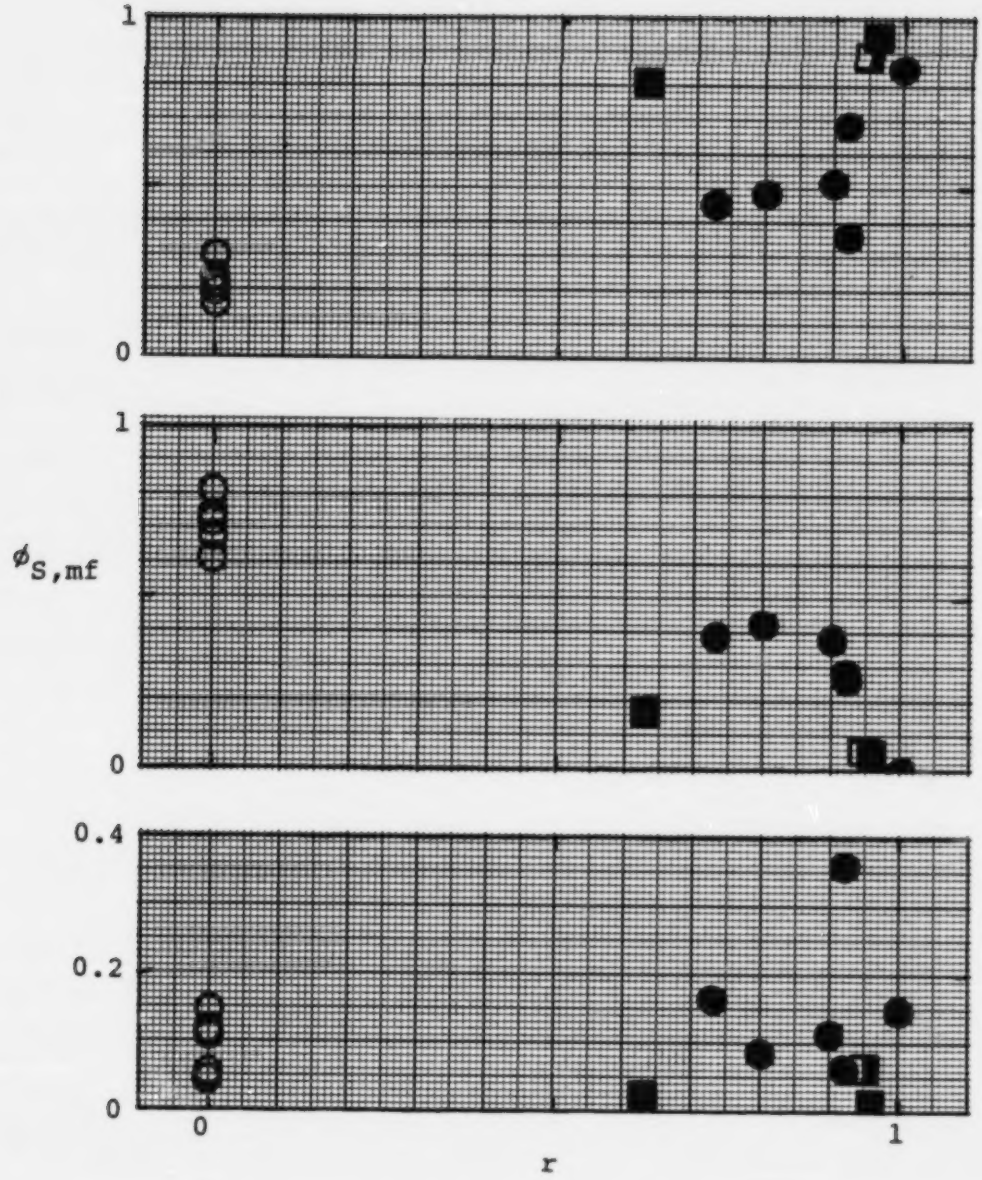

Fig. 6.6 Sulphur flux carried by the solid products, expressed as a fraction of fuel sulphur fed, vs recycle fraction: top, bed product; middle, cyclone product; bottom, baghouse product. Symbols: Table 4.2

7. Nitric oxide emission

Figure 7.1 shows the NO concentration in the stack gas as a function of the oxygen content of this gas. These quantities are often quite strongly correlated, showing decreasing NO level with decreasing O_2. Here, however, any such behaviour is not very evident. The range of the NO concentration is 180--400 ppm.

All our earlier studies, covering many fuels, have shown that the conversion factor

ξ_{NO} = fraction of fuel N converted to NO

is of more basic significance than the concentration of NO. It is typically in the range 0.10--0.25. The present results are unexceptional in this regard. Since freeboard reactions involving char are considered to be important in determining ξ_{NO}, it is interesting to examine it as a function of the freeboard carbon concentration estimated by $\dot{m}_{C,e}/A_b v$, Fig. 7.2. A particularly strong correlation is apparent for the trials with sand beds and recycle. These data are fitted by

$$\xi_{NO} = 0.38\, e^{-107\, \dot{m}_{C,e}/A_b v} \qquad (7.1)$$

An impressive correlation also exists, though, with the bed temperature, Fig. 7.3. Roughly,

$$\xi_{NO} = 0.1 + 0.001(T_b - 830), \qquad (7.2)$$

where T_b is in °C. Since freeboard carbon levels and bed temperature are considerably correlated, this result is not unexpected.

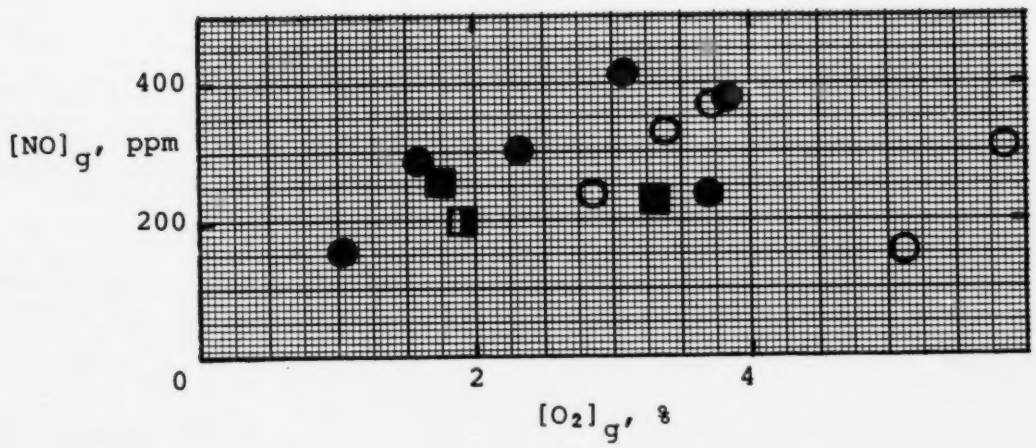

Fig. 7.1 Nitric oxide content of the exhaust gas vs the oxygen content. Symbols: Table 4.2

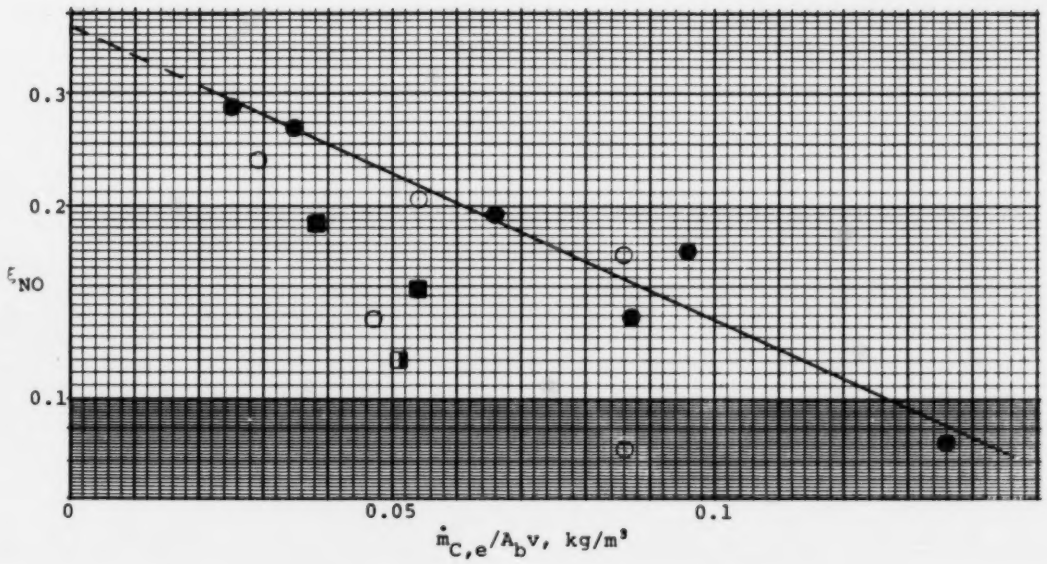

Fig. 7.2 Conversion of fuel nitrogen to nitric oxide vs concentration of unburnt carbon in the exhaust gas. Symbols: Table 4.2

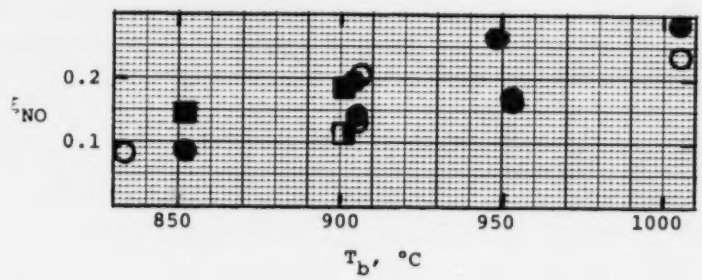

Fig. 7.3 Conversion of fuel nitrogen to nitric oxide vs bed temperature. Symbols: Table 4.2

8. Carbon monoxide emission

In past studies with other fuels we have found that CO levels in the stack gas are normally very low and almost constant until the stack-gas O_2 concentration drops below a critical value, whereupon the CO rises sharply. Figure 8.1 indicates similar results for the present case. The trials with recycle indicate CO levels of about 500 ppm at exhaust O_2 levels above 2 %. The results for operation without recycle indicate nearly the same result. At 1 % O_2, the CO level is about 1500 ppm.

9. Hydrogen in solid products

Figure 9.1 shows the molar H/C ratio of the cyclone and baghouse products. The hydrogen content of the bed product was generally too small for meaningful determination. It is seen that in all but two trials, the H/C ratio of the cyclone product was also very small, under 0.01. The H/C ratio of the baghouse product, however, was more elevated, 0.05--0.45 in all trials but one. In the exceptional trial, it was high in both baghouse and cyclone products, 0.85 in the former and 0.11 in the latter. The results suggest a tendency for H/C in the baghouse product to rise with bed temperature at temperatures above 850 °C.

10. Discussion

10.1 The effect of recycle on carbon loss

In the above treatment and in all our earlier work, we have characterized recycle by the cyclone recycle fraction r,

$$r = \dot{m}_r/(\dot{m}_r + \dot{m}_c) = \text{fraction of cyclone catch that is recycled}$$

This quantity is the controlled recycle variable, set by a variable splitter valve. In modelling the effect of recycle on

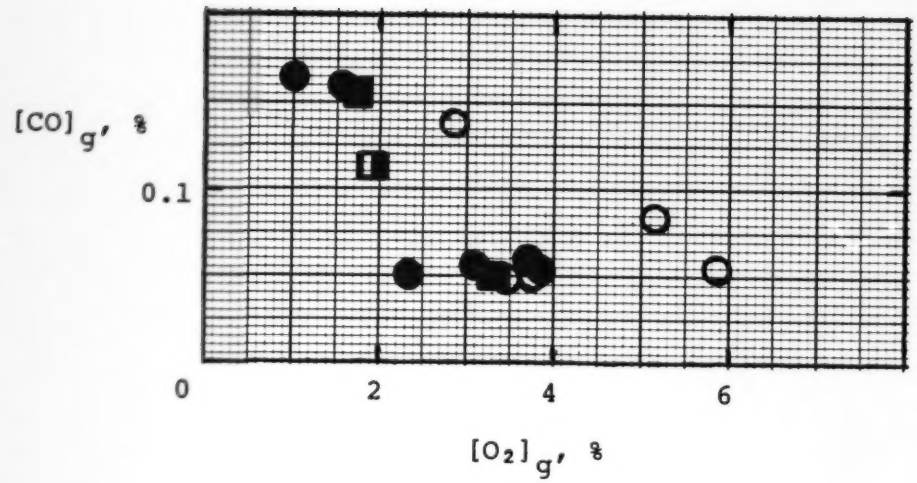

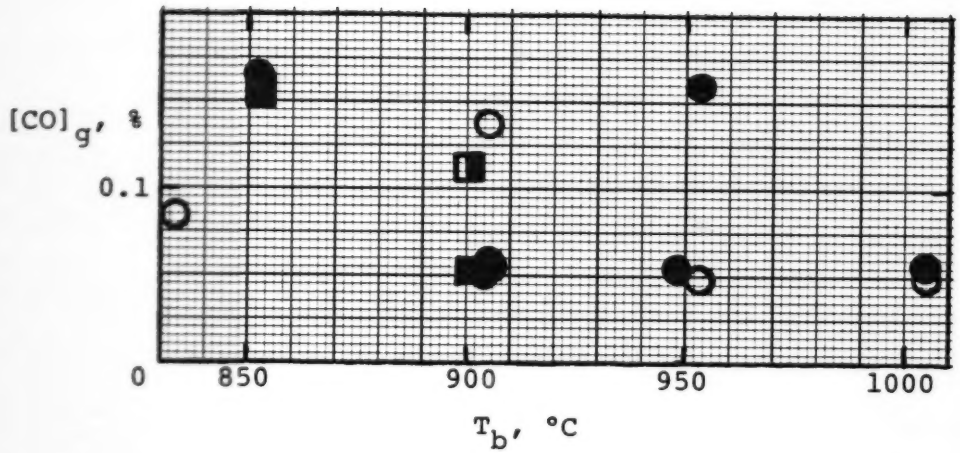

Fig. 8.1 Carbon monoxide content of the exhaust gas vs the oxygen content, top, and vs the bed temperature, bottom. Symbols: Table 4.2

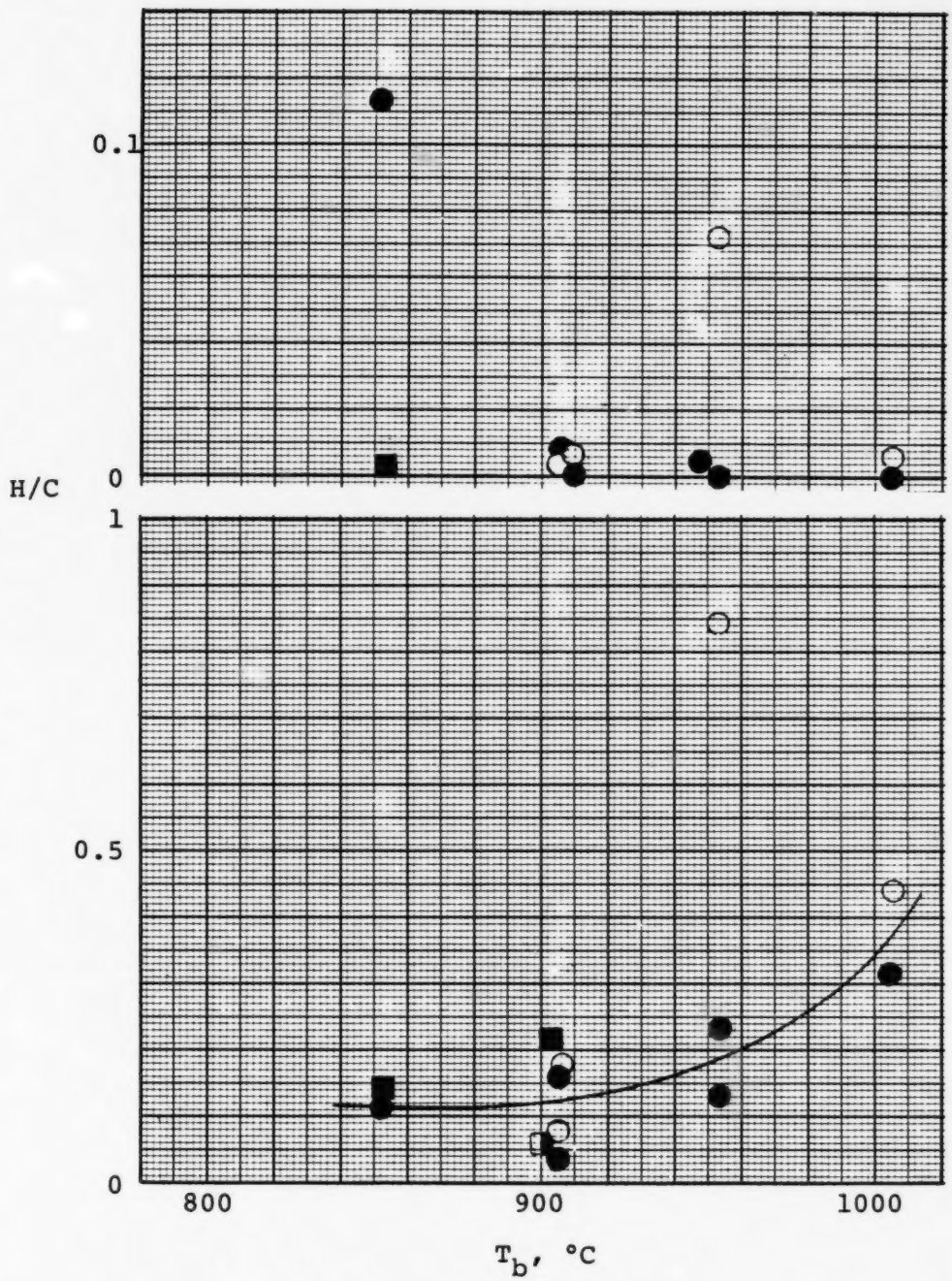

Fig. 9.1 Mole ratio of hydrogen to carbon in the solid products. Top, cyclone product; bottom, baghouse. Symbols: Table 4.2

carbon loss, it appeared that an exponential function, exp(ar), serves adequately and has reasonable properties; for example, exp(ar) = 1 at r = 0. As r → 1, we thought, the effect of recycle should weaken and reach a limit; this conjecture was, however, never critically examined. Because of the very great cyclone catches obtained then, frequently overloading and plugging our recycle system, we conducted very few trials at or very near r = 1. In the present work with sandbeds, the sand contained only a modest proportion of fines compared to the limestone products in trials with limestone. The elutriation of the sand and the resulting burden on the recycle system were correspondingly small. We were thus able to conduct some trials at r near unity, including one, 860226, at full cyclone recycle, r = 1. The carbon loss in that run was very low and far out of line with the other trials when correlated in terms of the recycle function exp(-ar). In a certain practical sense, such failure in prediction at very low carbon combustion inefficiencies does not matter; what is important is that the inefficiency be well predicted when it is substantial. Nevertheless, the possibility is raised that our handling of the effects of recycle may be generally improved if it is modified to give a better accounting of the case r = 1. Furthermore, such improvement may be of benefit to the development of the general theory of the modelling of fluidized bed combustion.

There are many measures available to express the intensity of recycle. One frequently seen in the literature is the ratio of recycle flux to coal feedrate, $\dot{m}_r/\dot{m}_f$. This may be of interest as an indicator of the relative loading of the solids transport systems but it has no clear significance as a factor affecting combustion efficiency and other operating characteristics of AFBC. It appears to us that the following parameters are most likely to be useful in this regard:

$r = \dot{m}_r/(\dot{m}_r + \dot{m}_c)$ = cyclone recycle fraction, the fraction of cyclone catch that is recycled, the measure we have hitherto used.

$\dot{m}_r/\dot{m}_c = r/(1 - r)$ = cyclone recycle ratio, the ratio of recycled cyclone catch to cyclone product

$R = \dot{m}_r/\dot{m}_e = \dot{m}_r/(\dot{m}_r + \dot{m}_c + \dot{m}_h)$ = overhead recycle fraction, the ratio of recycled solids to elutriated solids

$\dot{m}_r/(\dot{m}_c + \dot{m}_h) = R/(1 - R)$ = overhead recycle ratio, the ratio of recycled solids to overhead product (cyclone and baghouse)

Figure 10.1 shows the relationship between R and r for the present trials. The point for trial 860226, (r, R) = (1, 0.9917), is perforce omitted. For the data shown,

$$(1 - R) = (1 - r)^{0.925} \qquad (10.1)$$

gives a very good correlation. However, it is evident that at sufficiently small 1 - r this relation must fail. The relation between R and r clearly depends on the cyclone efficiency,

$$\eta_{cyc} = \frac{\dot{m}_d}{\dot{m}_e} = \frac{\dot{m}_r + \dot{m}_c}{\dot{m}_r + \dot{m}_c + \dot{m}_h} ,$$

and thus depends on the system characteristics, particularly those of the cyclone, and on the characteristics of the fuel and the stone. In the present case, η_{cyc} was generally high and so R and r are close to equality until r sufficiently nears unity, around r > 0.97 or higher.

We have considered the following recycle functions as substitutes for exp(ar):

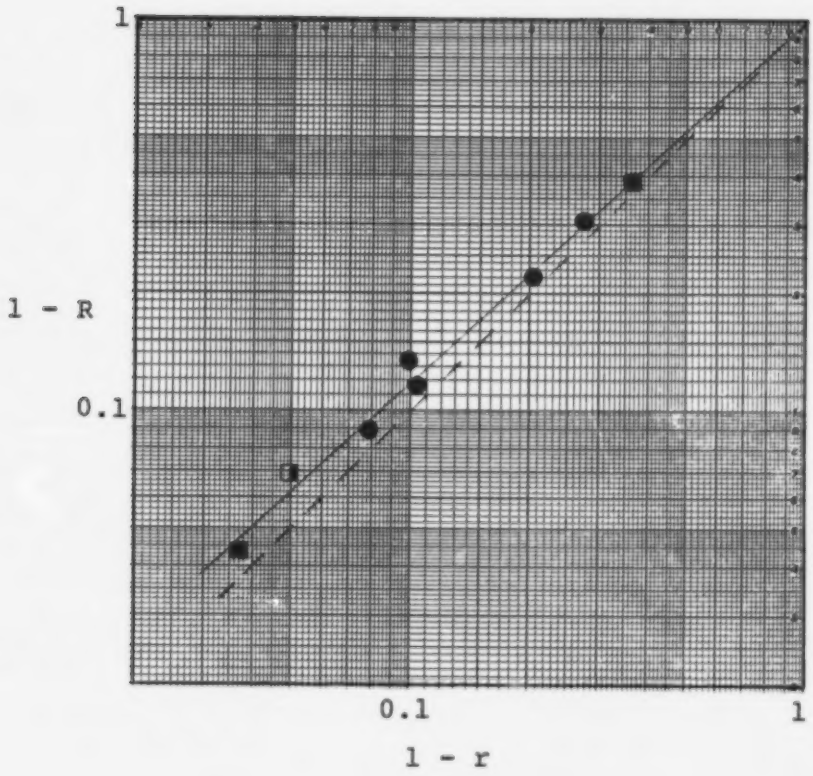

Fig. 10.1 Comparison of recycle functions. Dashed curve, $1 - R = 1 - r$; full curve, $1 - R = (1 - r)^{0.925}$. Symbols: Table 4.2

$$e^{ar/(1-r)}, \quad e^{aR/(1-R)}, \quad (1 - R)^a .$$

The first two are found to be much too strong as $r \to 1$ or $R \to 1$. The last, however, behaves appropriately. We accordingly replace $x_4 = a_4 r$ by $x_4 = a_4 \ln(1 - R)$ in the model (5.1) for regression analysis of carbon loss. The results obtained with the revised model, Table 10.1 and Fig. 10.2, are impressive. The fits for the trials other than 860226 are as good as the best from the old model, Table 5.2 and Fig. 5.10. In addition, the data for 860226, in which $r = 1$, are well accounted for.

We have, then, tentative evidence that the recycle function $(1 - R)^a$ is effective over the whole range of combustion inefficiency whereas the function $\exp(ar)$ is of limited utility. Table 10.2 and Fig. 10.3 show comparisons between these functions using best values of the coefficient a_4 from Tables 5.2 and 10.1. The difference is not great at $r < 0.90$, but at $r > 0.90$ the two functions diverge rapidly.

It thus appears that the function $(1 - R)^a$ is very likely better than $\exp(ar)$. We intend now to analyze again the results from all our earlier work using this new recycle function. We should then be able to draw some general conclusions.

The function $(1 - R)^a$ is attractive not only because it evidently provides better accounting of the case $r \to 1$, including $r = 1$, but because it would also permit, without discontinuity, treatment of operations where a part of the baghouse catch is recycled. In general, the recycle flux is simply the sum of the recycles from cyclone and baghouse. This puts AFBC systems on a common basis with RFBC (recirculating AFBC) systems. Recycle of baghouse catch is not normally employed in AFBC but it sometimes is in RFBC.

Table 10.1. Statistical fitting* of model for carbon loss, including effect of bed height and introducing the overhead recycle fraction R

$y = a_o + a_1x_1 + a_2x_2 + a_3x_3 + a_4x_4 + a_5x_5 + a_6x_6$,

$y = \ln (\dot{m}_{C,o}/\dot{m}_{C,f})$ for overhead carbon loss

$y = \ln (\dot{m}_{C,b}/\dot{m}_{C,f})$ for bed carbon loss

$a_o = \ln C$ $x_1 = \ln v$ $x_2 = \ln \hat{D}_{ps}$ $x_3 = \ln \phi_a$

$x_4 = \ln (1 - R)$ $x_5 = 1/T_b$ $x_6 = \ln H$

	a_o	C	a_1	a_2	a_3	a_4	a_5	a_6		
	s_o		s_1	s_2	s_3	s_4	s_5	s_6	s_y	R^2
Overhead loss, all trials	-5.30	0.0050	0.49	-1.83	-2.74	0.82	4087	0.80		
	3.35		0.77	0.75	1.20	0.07	3078	0.83	0.28	0.980
Overhead loss, sand beds	-4.27	0.014	0.27	0	-2.90	0.78	4186	0.93		
			0.86	--	1.33	0.09	3356	0.91	0.30	0.979
	-3.65	0.026	0	0	-2.90	0.77	3688	1.02		
			--	--	1.23	0.07	2740	0.80	0.28	0.978
Bed loss, all trials	-10.92	0.000018	-1.11	-0.03	-1.06	0.12	3078	-3.31		
	11.32		2.61	2.54	4.05	0.25	10400	2.81	0.94	0.36
Bed loss, sand beds	-12.49	0.000004	-0.58	0	-0.05	0.24	4262	-3.85		
	11.83		3.00	--	4.64	0.31	11675	3.17	1.04	0.41
	-13.85	0.000001	0	0	0	0.27	5376	-4.01		
	6.86		--	--	--	0.19	7428	2.37	0.88	0.40
	-9.15	0.00011	0	0	0	0.29	0	-3.87		
	2.12		--	--	--	0.18	--	2.29	0.86	0.36

*s_i = standard error of estimate of a_i

s_y = standard error of prediction of y

R^2 = coefficient of multiple correlation (no relation to the overhead recycle fraction R)

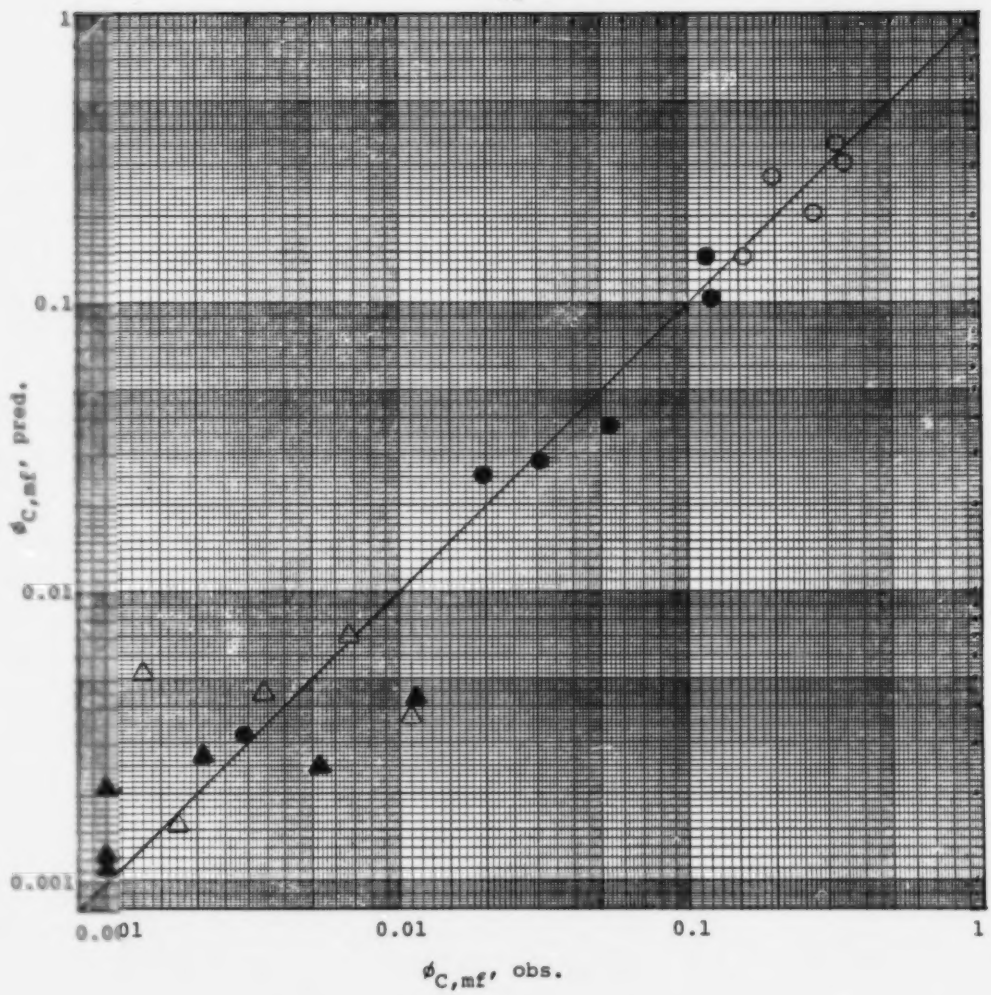

Fig. 10.2 Predicted carbon loss vs that measured, both normalized on fuel carbon fed, for all trials with sand beds. Prediction from the models in Table 10.2 for overhead carbon loss (○, ●), independent variable set (ϕ_a, R, T_b, H), and bed carbon loss (△, ▲), independent variable set (R, T_b, H). Cyclone recycle fraction r: ○△, 0; ● ▲, 0.73--1

Table 10.2. Comparison of recycle functions

Trial	r	R	$e^{-1.6r}$	$(1 - R)^{0.8}$
five	0	0	1	1
860303	0.797	0.780	0.279	0.298
860304	0.921	0.901	0.229	0.157
860311	0.728	0.694	0.312	0.388
860219	0.898	0.885	0.238	0.177
860226	1	0.9917	0.202	0.022
860225	0.902	0.867	0.236	0.199
860317	0.633	0.615	0.363	0.466
860318	0.963	0.956	0.214	0.082
860324	0.951	0.931	0.218	0.118
Synthetic,	0.2	0.2	0.726	0.837
set r = R	0.4	0.4	0.527	0.665
	0.6	0.6	0.383	0.480
	0.8	0.8	0.278	0.276
	0.9	0.9	0.237	0.158
	0.95	0.95	0.219	0.091
	0.98	0.98	0.208	0.044

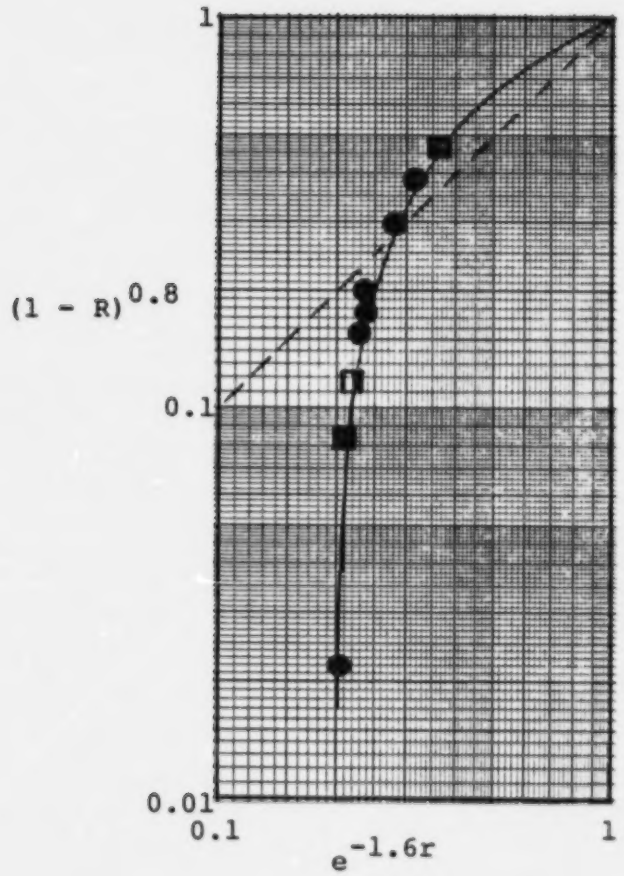

Fig. 10.3 Comparison of recycle functions. Full curve: the case r = R. Symbols: Table 4.2

10.2 Comparison of carbon loss with the Syncrude trials

In our AFBC pilot-plant studies of the combustion of Syncrude coke, eight successful trials were carried out. The same Athabasca limestone used in the present work was employed, in two sizes: $\hat{D}_{ps}$ = 0.34 mm and 0.94 mm. The mass-median fuel particle diameter, $\hat{D}_{pf}$ = 0.26 mm, is similar to the present coke. Ranges of other key operating variables are Ca/S = 1.7--2.9, ϵ_a = -28--7 %, r = 0--0.83, T_b = 966--1105 °C, and v = 0.8--1.3 m/s. Bed temperature and recycle were found to be by far the strongest variables and a good correlation of overhead carbon loss was given by

$$m_{C,o}/m_{C,f} = 0.00041\, e^{-1.79r}\, e^{7600/T_b} \qquad (10.1)$$

The temperature effect in this result is considerably stronger than in the present work, Tables 5.2 and 10.1: a_5 = 7600 K compared to $a_5 \simeq$ 4000 K. However, the difference is within the estimated standard error of a_5. The recycle effect, on the other hand, appears to be either a little weaker or about the same; in exp (a_4r), a_4 = -1.79 compared to $a_4 \simeq$ -(1.7--2.5). The difference again is within the estimated standard error.

To compare the Syncrude results with those on the present coke, we have calculated predicted overhead carbon losses from (10.1) for the present conditions. Figure 10.4 shows the ratio of the predicted and observed losses as a function of the recycle fraction r. The agreement is well within the confidence limits of (10.1) up to r = 0.90. The predicted value thereafter rapidly increases over the actual, reaching a ratio of 12 at r = 1. This behaviour supports the conclusions about effects of recycle presented in Sect. 10.1; the function exp (a_4r) is inadequate at r $\geq$ 0.90 and then greatly overpredicts the overhead carbon loss. Replacement by the function $(1-R)^{a_4}$ solves this problem. The

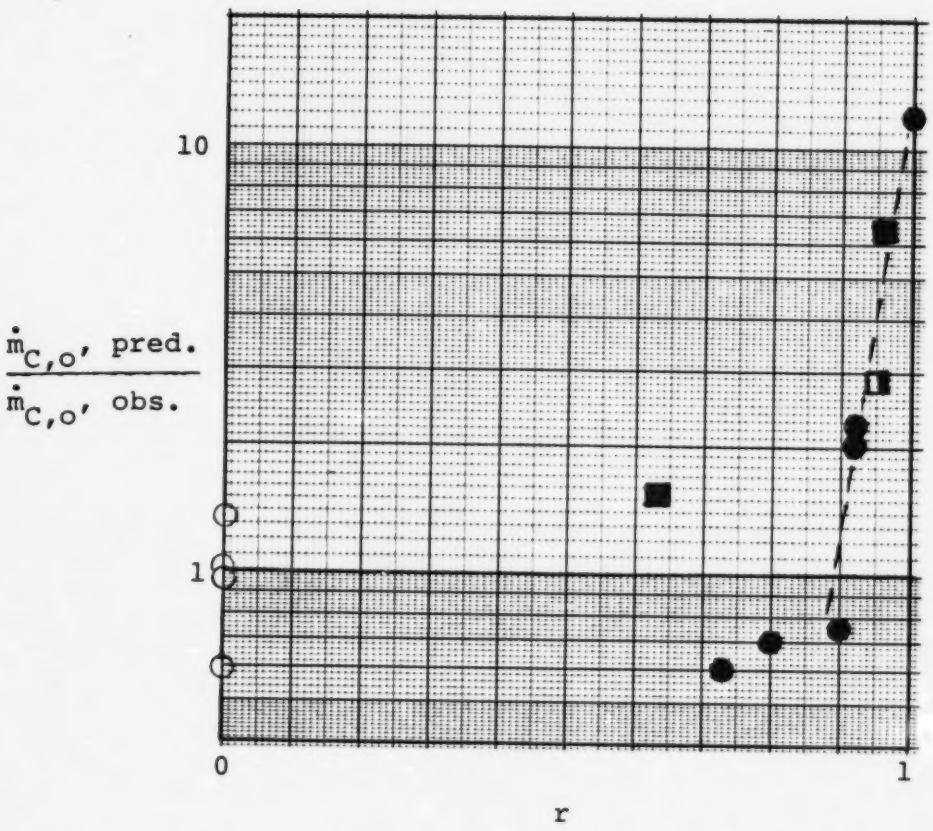

Fig. 10.4 Overhead carbon loss predicted by the "Syncrude correlation", (10.1), divided by that observed in the present trials, vs cyclone recycle fraction. Symbols: Table 4.2

Syncrude trials only extended up to r = 0.83 and so this difficulty was not evident from them.

10.3 Sulphur removal by elutriated char

The concentration of sulphur in unburnt char has been observed in previous work where sand beds were used. In our trials with Mt. Klappan anthracite coal (Becker, Code & Stephenson 1987a), combustion efficiencies were generally low. In several trials, the combustion inefficiency was 18--22 %. The total sulphur in the bed products was about 65% of the fuel sulphur. This shows an increase in the S/C mole ratio by a factor of over 3. In trials with Highvale sub-bituminous coal (Becker, Code & Stephenson 1987b), however, the coal had a natural Ca/S ratio of 3.7 and the retention of sulphur in unburnt char was effectively masked by its capture in $CaSO_4$.

It seems reasonable to strongly suspect that in all fluidized bed combustion, sulphur is retained in unburnt char where its content, in terms of the S/C mole ratio, is concentrated relative to the parent fuel. This complicates the modelling of sulphur capture, particularly in cases of moderate or poor combustion efficiency. We shall accordingly re-examine the results of our past trials on coal combustion to evaluate the likely effects of this factor.

10.4 Nitric oxide emission

The nitric oxide emissions seen in the present work, indicating 10--25 % conversion of fuel nitrogen to NO, are typical of AFBC in our experience and unremarkable in that sense. Since the fuel nitrogen was, however, high, the absolute emission levels (150--400 ppm) might nevertheless be of concern. There is clearly a premium on low nitrogen content in fuels for AFBC.

11. Conclusion

The present work suggests that petroleum cokes tend to have combustion behaviour determined by particle size and little more. Two cokes of very dissimilar origin--the present coke from processing light Alberta crude oil and Syncrude coke from processing Alberta oil sands--are well described by the same correlation. Such cokes have the simplifying characteristic that they do not swell on heating and are not prone to fragmentation.

The second major finding is the role of unburnt carbon in sulphur "capture". Sulphur evidently concentrates in the char and may in it reach S/C mole ratios up to three times those in the parent fuel. That some sulphur must be retained in the unburnt char is self-evident. We have not, however, in our past work recognized that this effect can have a significant role in apparent sulphur "capture".

References

Anthony, E.J., Becker, H.A., Code, R.K., McCleave, R.W. and Stephenson, R.J. 1987, "Bubbling Fluidized Bed Combustion of Syncrude Coke", Proc. 1987 International Conference on Fluidized Bed Combustion, Vol. 1, 322--329, The American Society of Mechanical Engineers

Becker, H.A. and Code, R.K. 1982, The Pilot Plant Installation at Queen's University for Studies of Atmospheric Fluidized Bed Combustion. Report QFBC.TR.82.1, Queen's Fluidized Bed Combustion Laboratory, Department of Chemical Engineering, Queen's University, Kingston, Canada K7L 3N6

Becker, H.A. and Code, R.K. 1983, Pilot Plant Trials on Atmospheric Fluidized Bed Combustion of High-Sulphur Eastern Canadian Coals (Minto and Devco) with Limestone Addition for Sulphur Capture. Report to Energy Mines and Resources, Canada, CANMET, Ottawa. Report QFBC.TR.83.1, Queen's Fluidized Bed Combustion Laboratory, Department of Chemical Engineering, Queen's University, Kingston, Canada K7L 3N6

Becker, H.A., Code, R.K., McCleave, R.W. and Stephenson, J.R. 1985, Pilot Plant Studies of Fluidized Coal Combustion. Report to Energy Mines and Resources Canada, CANMET, Ottawa. Report QFBC.TR.85.1, Queen's Fluidized Bed Combustion Laboratory, Department of Chemical Engineering, Queen's University, Kingston, Canada K7L 3N6

Becker, H.A., Code, R.K. and Stephenson, J.R. 1987a, Pilot Scale Trials on Atmospheric Fluidized Bed Combustion of a Western Canadian Sub-bituminous Coal (Highvale), Technical Report QFBC.TR.87.3, Queen's Fluidized Bed Combustion Laboratory. Prepared for Energy, Mines and Resources Canada, Energy Research Laboratories, CANMET, as the Final Report on the Highvale trials, DSS Contract OST84-00512

Becker, H.A., Code, R.K. and Stephenson, J.R. 1987b, "Pilot-Scale Trials on Atmospheric Fluidized Bed Combustion of British Columbian Anthracite (Mt. Klappan)", Technical Report QFBC.TR.87.4, Queen's Fluidized Bed Combustion Laboratory. Prepared for Energy, Mines and Resources Canada, Energy Research Laboratories, CANMET as the Final Report on the petroleum coke trials, DSS Contract OST84-00512

Friedrich, F.D., Lee, G.K., Desai, D.L. and Kuivaleinin, R. 1982, "Fluidized-bed combustion of petroleum coke", Joint Power General Conference, Denver, Colorado, October 1982, sponsored by the ASME